doi:10.1093/brain/awu046 Brain 2014: 137; 1533–1549 | 1533

BRAIN
A JOURNAL OF NEUROLOGY

Regional distribution of synaptic markers and APP correlate with distinct clinicopathological features in sporadic and familial Alzheimer's disease

Mitsuru Shinohara,[1] Shinsuke Fujioka,[1,2] Melissa E. Murray,[1] Aleksandra Wojtas,[1] Matthew Baker,[1] Anne Rovelet-Lecrux,[3] Rosa Rademakers,[1] Pritam Das,[1] Joseph E. Parisi,[4] Neill R. Graff-Radford,[2] Ronald C. Petersen,[5] Dennis W. Dickson[1] and Guojun Bu[1]

1 Department of Neuroscience, Mayo Clinic, Jacksonville, FL, USA
2 Department of Neurology, Mayo Clinic, Jacksonville, FL, USA
3 Inserm U1079, Institute for Research and Innovation in Biomedicine, University of Rouen, France
4 Department of Laboratory Medicine and Pathology, Mayo Clinic, Rochester, MN, USA
5 Department of Neurology, Mayo Clinic, Rochester, MN, USA

Correspondence to: Guojun Bu, Ph.D.,
Department of Neuroscience,
Mayo Clinic, 4500 San Pablo Road,
Jacksonville, FL 32224, USA
E-mail: bu.guojun@mayo.edu

Recent studies suggest that subcortical structures, including striatum, are vulnerable to amyloid-β accumulation and other neuropathological features in familial Alzheimer's disease due to autosomal dominant mutations. We explored differences between familial and sporadic Alzheimer's disease that might shed light on their respective pathogenic mechanisms. To this end, we analysed 12 brain regions, including neocortical, limbic and subcortical areas, from post-mortem brains of familial Alzheimer's disease ($n = 10$; age at death: 50.0 ± 8.6 years) with mutations in amyloid precursor protein (*APP*) or presenilin 1 (*PSEN1*), sporadic Alzheimer's disease ($n = 19$; age at death: 84.7 ± 7.8 years), neurologically normal elderly without amyloid-β accumulation (normal ageing; $n = 13$, age at death: 82.9 ± 10.8 years) and neurologically normal elderly with extensive cortical amyloid-β deposits (pathological ageing; $n = 15$; age at death: 92.7 ± 5.9 years). The levels of amyloid-β_{40}, amyloid-β_{42}, APP, apolipoprotein E, the synaptic marker PSD95 (now known as DLG4), the astrocyte marker GFAP, other molecules related to amyloid-β metabolism, and tau were determined by enzyme-linked immunosorbent assays. We observed that familial Alzheimer's disease had disproportionate amyloid-β_{42} accumulation in subcortical areas compared with sporadic Alzheimer's disease, whereas sporadic Alzheimer's disease had disproportionate amyloid-β_{42} accumulation in cortical areas compared to familial Alzheimer's disease. Compared with normal ageing, the levels of several proteins involved in amyloid-β metabolism were significantly altered in both sporadic and familial Alzheimer's disease; however, such changes were not present in pathological ageing. Among molecules related to amyloid-β metabolism, the regional distribution of PSD95 strongly correlated with the regional pattern of amyloid-β_{42} accumulation in sporadic Alzheimer's disease and pathological ageing, whereas the regional distribution of APP as well as β-C-terminal fragment of APP were strongly associated with the regional pattern of amyloid-β_{42} accumulation in familial Alzheimer's disease. Apolipoprotein E and GFAP showed negative regional association with amyloid-β (especially amyloid-β_{40}) accumulation in both sporadic and familial Alzheimer's disease. Familial Alzheimer's disease had greater striatal tau pathology than sporadic Alzheimer's disease. In a retrospective medical record review, atypical signs and symptoms were more frequent in familial Alzheimer's disease compared with sporadic Alzheimer's disease. These results suggest that disproportionate amyloid-β_{42} accumulation in cortical areas in sporadic Alzheimer's disease may be mediated by synaptic processes, whereas disproportionate amyloid-β_{42} accumulation in subcortical areas in familial Alzheimer's disease may be driven by APP and its processing.

Received October 28, 2013. Revised January 4, 2014. Accepted January 20, 2014. Advance Access publication March 12, 2014

Region-specific amyloid-β_{42} accumulation might account for differences in the relative amounts of tau pathology and clinical symptoms in familial and sporadic Alzheimer's disease.

Keywords: Alzheimer's disease; amyloid-β; neuroanatomy; APP; synapses

Abbreviation: GuHCl = guanidine hydrochloride

Introduction

Neuropathological hallmarks of Alzheimer's disease, the most common form of dementia in elderly, include amyloid-β and tau accumulation, which appear as senile plaques and neurofibrillary tangles or dystrophic neuritis, respectively. Although most cases of Alzheimer's disease are the sporadic, late-onset form (so-called 'sporadic Alzheimer's disease'), a small proportion (~1%) are characterized as autosomal dominant, early-onset Alzheimer's disease (so-called 'familial Alzheimer's disease') (Thies and Bleiler, 2013). It is well known that almost all familial Alzheimer's disease-linked genetic mutations upregulate the cellular production of amyloid-β_{42}, or increase the ratio of amyloid-β_{42} to amyloid-β_{40} (Citron *et al*., 1992; Duff *et al*., 1996; Scheuner *et al*., 1996). Moreover, increased ratio of production of amyloid-β_{42} to amyloid-β_{40} is associated with an earlier age of onset in familial Alzheimer's disease as a result of presenilin mutations (Duering *et al*., 2005; Kumar-Singh *et al*., 2006). These findings strongly support the amyloid cascade hypothesis in the pathogenesis of Alzheimer's disease (Karran *et al*., 2011).

Although familial Alzheimer's disease is known to be caused by mutations in the genes of amyloid precursor protein (*APP*) presenilin 1 (*PSEN1*) or presenlin 2 (*PSEN2*), it remains unclear how disturbances in amyloid-β metabolism—overproduction or inefficient clearance of amyloid-β leading to its accumulation—are involved in the pathogenesis of sporadic Alzheimer's disease. Proteolytic cleavage of APP by β-site cleaving enzymes and subsequent cleavage of β-C-terminal fragment of APP (APP-CTFβ) by γ-secretase produce amyloid-β (Thinakaran and Koo, 2008). Upon production, much of amyloid-β is efficiently cleared by amyloid-β degrading enzymes, cellular uptake to lysosomes, or brain vasculature. Cellular clearance of amyloid-β by various cell types in brain parenchyma and vasculature is mediated by cell surface amyloid-β-binding receptors and is regulated by apolipoprotein E (apoE) (Bu, 2009). Synapses are thought to be involved in both production and clearance of amyloid-β (Shigematsu *et al*., 1992; Takahashi *et al*., 2002; Cirrito *et al*., 2005; Koffie *et al*., 2009; Wu *et al*., 2011).

An analysis of region-specific amyloid-β accumulation can provide important insights into the pathomechanisms of Alzheimer's disease (Buckner *et al*., 2005; Bero *et al*., 2011; Shinohara *et al*., 2013). Neuropathological staging suggests that amyloid-β deposition occurs first in neocortical areas, followed by limbic areas, and then subcortical areas and the cerebellum (Thal *et al*., 2002; Rowe *et al*., 2007). On the other hand, emerging evidence from recent amyloid imaging studies indicates that subcortical areas, such as the striatum and thalamus, are more vulnerable to amyloid-β accumulation during early stages of familial Alzheimer's disease (Klunk *et al*., 2007; Koivunen *et al*., 2008; Remes *et al*., 2008; Villemagne *et al*., 2009; Knight *et al*., 2011). Though it is not yet clear whether such differences in region-specific amyloid-β accumulation impact neuropathological processes and clinical symptoms, recent functional MRI studies provide evidence of neurodegeneration in subcortical areas in presymptomatic stages of familial Alzheimer's disease due to *PSEN1* mutations (Lee *et al*., 2013; Ryan *et al*., 2013). Of note, several case studies of familial Alzheimer's disease had noted frequent atypical clinical signs and symptoms, some of which could be associated with subcortical dysfunction (Rossor *et al*., 1993; Cabrejo *et al*., 2006; Larner and Doran, 2006, 2009).

We aimed to elucidate the mechanism underlying such distinct region-specific clinicopathological features in sporadic and familial Alzheimer's disease. Based on our previous studies in the biochemical analysis of regional differences in levels of amyloid-β and molecules related to amyloid-β metabolism in non-demented individuals (Shinohara *et al*., 2013), we hypothesized that there were similarities and differences in the neuroanatomical relationship between amyloid-β and molecules related to amyloid-β metabolism in sporadic Alzheimer's disease, familial Alzheimer's disease, and non-demented individuals. In particular, when considering the pathological relationship between amyloid-β accumulation and neurodegeneration (Jack *et al*., 2013), comparisons among different disease states related to the degree of amyloid-β accumulation [i.e. (i) non-disease state, neurologically normal without amyloid-β accumulation; (ii) prodromal disease state, neurologically normal with amyloid-β accumulation; and (iii) disease state] would be critical to understanding pathogenic mechanisms involved in amyloid-β accumulation during disease development (Shinohara and Bu, 2013). Therefore, in this study, we assessed regional distribution of amyloid-β accumulation, and molecules related to amyloid-β metabolism, in post-mortem brains from individuals who were neurologically normal with or without amyloid-β accumulation and those with sporadic Alzheimer's disease or familial Alzheimer's disease as a result of *APP* or *PSEN1* mutations. We also evaluated tau accumulation using biochemical and digital imaging microscopy and compiled ante-mortem clinical symptoms in sporadic and familial Alzheimer's disease by retrospective review of medical records.

Materials and methods

Sample material

Post-mortem tissues were obtained through the Mayo Clinic Brain Bank for neurodegenerative diseases, whose operating procedures

Table 1 Demographic characteristics of cohorts

Cohort	*n*	Age at death (years)	Male:female	Braak NFT stage	Disease duration (years)	Post-mortem interval (h)	Cortical Aβ40 level in GuHCl (ng/mg)	Cortical Aβ42 level in GuHCl (ng/mg)
Normal ageing	13	82.9 ± 10.8 (57–97)	4:9	II (0–IV)	-	12.7 ± 4.2 (5–18)	1.1 ± 0.2	2.0 ± 0.5
Pathological ageing	15	92.7 ± 5.9 (82–101)	2:13	III (I–IV)	-	10.5 ± 6.2 (2–23)	14.0 ± 8.5*,†	106.1 ± 18.4**
SAD	19	84.7 ± 7.8 (62–95)	5:14	VI$^{*,\#}$ (V–VI)	10.4 ± 3.7 (6–17)	10.7 ± 7.7 (2–24)	99.4 ± 52.2**	102.5 ± 8.9**
FAD	10	50 ± 8.6$^{*,\#,\S}$ (37–64)	5:5	VI$^{*,\#}$ (VI–VI)	6.4 ± 3.0§ (4–13)	14.4 ± 14.0 (3–36)	70.8 ± 22.3**	82.4 ± 15.4**

Values are mean ± SD (range) for age at death, disease duration and post-mortem interval.
Values are mean ± SE for cortical amyloid-β_{40} level in GuHCl and cortical amyloid-β_{42} level in GuHCl.
Values are median (range) for Braak NFT stage, and number of subjects.
$^{*}P < 0.05$, $^{**}P < 0.01$; compared with normal ageing by *post hoc* Dunn's test.
$^{\#}P < 0.05$, $^{\#\#}P < 0.01$; compared with pathological ageing by *post hoc* Dunn's test.
$^{\S}P < 0.05$; compared with sporadic Alzheimer's disease by *post hoc* Dunn's test.
$^{\dagger}P = 0.063$; compared with sporadic Alzheimer's disease, $P = 0.077$; compared with familial Alzheimer's disease by *post hoc* Dunn's test.
Aβ = amyloid-β; FAD = familial Alzheimer's disease; NFT = neurofibrillary tangles; SAD = sporadic Alzheimer's disease.

are approved by the Mayo Institutional Review Board. In addition to sporadic and familial Alzheimer's disease, we also evaluated neurologically normal elderly subjects without amyloid-β accumulation (normal ageing) and neurologically normal elderly subjects with extensive cortical amyloid-β deposits (pathological ageing) (Dickson *et al*., 1992). All normal ageing, pathological ageing and sporadic Alzheimer's disease cases were from the Mayo Clinic Alzheimer Disease Research Centre (ADRC; P50 AG016574) or Mayo Clinic Study of Ageing (MCSA; U01 AG006786), whereas cases with familial Alzheimer's disease were from a range of referral sources. The normal ageing, pathological ageing and sporadic Alzheimer's disease cases had standardized neurological and neuropsychological assessment through the Mayo Clinic Alzheimer Disease Research Centre and Mayo Clinic Study of Ageing, but cases with familial Alzheimer's disease did not have systematic evaluations. Sequencing of *APP*, *PSEN1* and *PSEN2* was performed in all cases with early-onset Alzheimer's disease using methods as previously described (Wojtas *et al*., 2012). Genomic *APP* copy-number analysis was performed using real-time PCR and confirmed by QMPSF (quantitative multiplex PCR of short fluorescent fragments) analysis (Rovelet-Lecrux *et al*., 2006). Demographic characteristics of the cases and individual genetic mutations in cases with familial Alzheimer's disease are shown in Tables 1 and 2, respectively.

Sample preparation

Grey matter of 12 brain areas (Table 3) was dissected and kept frozen until extraction. Brain lysates were prepared by the three-step extraction method based upon differential solubility in detergents (Triton^{TM} X-100) and chaotropic agents [guanidine hydrochloride (GuHCl)] as previously described (Shinohara *et al*., 2013). In brief, after removal of meninges and blood vessels, 100–200 mg of frozen brain tissue were homogenized in ice-cold TBS containing a protease inhibitor cocktail (Roche Diagnostics) by Polytron homogenizer (KINEMATICA). After centrifugation at 100 000*g* for 60 min at 4°C, the supernatant was aliquoted and stored at −80°C (referred to as TBS fraction or TBS). The residual pellet was rehomogenized in TBS plus 1% Triton^{TM} X-100 with protease inhibitor cocktail, incubated with mild agitation for 1 h at 4°C and centrifuged as above. The resultant supernatant was aliquoted and stored at −80°C (referred to as TX fraction or TX). The residual pellet was rehomogenized in TBS plus 5 M GuHCl, pH 7.6, and incubated with mild agitation for 12–6 h at 22°C. After centrifugation as above, the resultant supernatant (referred to as the GuHCl fraction) was diluted with nine volumes of TBS, aliquoted and stored at −80°C.

Quantification of proteins

Levels of total proteins, amyloid-β_{1-40}, amyloid-β_{1-42}, APP, APP-CTFβ, β-site cleaving enzyme 1 (BACE1), presenilin 1 (PSEN1), APOE, insulin degrading enzyme (IDE), neprilysin (NEP, now known as MME), low-density lipoprotein receptor (LDLR), LDLR-related protein 1 (LRP1), glial fibrillary acidic protein (GFAP), synaptophysin (SYP), and postsynaptic density 95 (PSD95, now known as DLG4) were determined by ELISAs as previously described (Shinohara *et al*., 2013). Levels of tau were determined by ELISA using a rabbit anti-C-terminus of tau capture antibody (Osenses) and biotin-conjugated mouse monoclonal HT7 detector antibody (epitope between amino acids 159–163, Thermo scientific). Recombinant human tau proteins (Millipore) were used as standards. Colorimetric quantification was performed on a Synergy HT plate reader (BioTek) using horseradish peroxidase (HRP)-linked streptavidin (Vector) or Poly-HRP 40 streptavidin (Fitzgerald) and 3,3′,5,5′-tetramethylbenzidine substrate (Sigma). Levels of specific proteins were determined on one of the three fractions, based on their abundance among these fractions, by using small samples derived from both normal controls and cases with Alzheimer's disease. Specifically, the TBS fraction was used to measure levels of cytosolic/secreted proteins and molecules (i.e. IDE, GFAP, and PSD95). The TX fraction was used to measure levels of membrane proteins (i.e. APP, APP-CTFβ, BACE1, PSEN1, NEP, LDLR, LRP1, and SYP). The GuHCl fraction was used to measure levels of pathological aggregated proteins amyloid-β_{1-40}, amyloid-β_{1-42}, and tau. ApoE levels were determined in all fractions, as we found the abundance of this protein in each fraction differs between normal control subjects and cases with Alzheimer's disease.

Immunohistochemistry and image analysis of tau

Striata of sporadic and familial Alzheimer's disease were immunostained with two phosphorylated tau antibodies, CP13 (pSer202) and PHF1 (pSer396-pSer404) (both from Peter Davies, Albert Einstein College of Medicine). CP13 recognizes early pretangles and intracellular tangles, whereas PHF1 recognizes more advanced neurofibrillary degeneration, including some extracellular tangles in addition to pretangles and intracellular tangles. Immunostained slides were scanned on an Aperio ScanScope XT slide scanner (Aperio Technologies) producing high-resolution digital images. Annotation of regions of interest was performed using Aperio ImageScope software. Two colour deconvolution algorithms were designed to detect the optical density and

Table 2 Individual genetic mutation of cases with familial Alzheimer's disease

Carrier	Mutation	Age at death (year)	Gender	Braak NFT stage	Cortical amyloid-β_{40} level in GuHCl fraction (ng/mg)	Cortical amyloid-β_{42} level in GuHCl fraction (ng/mg)
APP	Duplication	50	F	VI	197.4 ± 44.5	52.2 ± 3.1
PSEN1	I143T	38	F	VI	9.8 ± 2.9	195.9 ± 6.5
PSEN1	Y288F	51	M	VI	134.6 ± 43.3	55.5 ± 9.8
PSEN1	L392V	50	M	VI	137.9 ± 62.5	121.0 ± 18.4
PSEN1	N135S	44	M	VI	25.6 ± 6.5	33.9 ± 3.0
PSEN1	N135S	37	F	VI	17.0 ± 8.9	39.1 ± 3.4
PSEN1	N135S	57	F	VI	47.8 ± 11.4	52.1 ± 4.8
PSEN1	G378V	51	F	VI	12.1 ± 2.9	90.2 ± 20.3
PSEN1	G206A	64	M	VI	123.3 ± 33.7	86.8 ± 8.7
APP	V717F	58	M	VI	2.6 ± 0.5	97.9 ± 10.2

Values are mean ± SE for cortical amyloid-β_{40} level in GuHCl fraction and cortical amyloid-β_{42} level in GuHCl fraction.
NFT = neurofibrillary tangles; F = female; M = male.

intensity threshold of the diaminobenzidene chromogen in the striatum for both CP13 and PHF1 (Janocko *et al.*, 2012). The output variable was percentage of strong positive staining (based on area of the region of interest).

Data analysis

All measured values by ELISAs were first normalized by total protein levels in the sample. Comparisons of demographic features as well as cortical protein levels (averaged value of cortical areas) among multiple cohorts were performed by Kruskal-Wallis one-way ANOVA on ranks, with all pairwise comparisons using Dunn's test (SigmaPlot, version 11.0; Systat Software Inc). To assess region-specific difference, each measured value normalized by total protein levels was then normalized by the average value within an individual to adjust for the influence of difference between individuals. Comparisons of such normalized values between two cohorts were performed by Wilcoxon rank-sum test (JMP Pro, version 9; SAS). The non-parametric Spearman rank correlation coefficient (JMP) was used to summarize the degree of correlation between median levels of each protein (normalized value within individual) across 12 brain regions (Shinohara *et al.*, 2013). *P*-values < 0.05 were considered significant.

Results

Comparison of regional distribution of amyloid-β between sporadic and familial Alzheimer's disease

In this study, we focused on analysing insoluble amyloid-β (i.e. amyloid-β in the GuHCl fraction) rather than soluble amyloid-β (i.e. amyloid-β in the TBS and TX fractions), as amyloid-β in the insoluble fraction represents the vast majority of all accumulated amyloid-β in sporadic and familial Alzheimer's disease (Supplementary Table 1). In comparing levels of accumulated amyloid-β in sporadic and familial Alzheimer's disease, we found no significant differences in the absolute amounts as shown by the average values across cortical regions (Table 1). However, when we compared absolute amounts of accumulated amyloid-β in each region, we found differences in specific brain regions (Supplementary Fig. 1). As these differences could include both interindividual variability and regional variability, we used regional values normalized within each individual to assess whether sporadic and familial Alzheimer's disease exhibit region-specific neuroanatomical differences in amyloid-β accumulation. Indeed, familial Alzheimer's disease had disproportionate accumulation of amyloid-β_{40}, compared to sporadic Alzheimer's disease, in the cerebellum (Fig. 1A). Moreover, several neocortical areas (dorsolateral prefrontal cortex, inferior temporal cortex and inferior parietal cortex) and one limbic area (posterior cingulate) had disproportionate amyloid-β_{42} accumulation in sporadic Alzheimer's disease compared with familial Alzheimer's disease. In contrast, all subcortical areas and one limbic area (amygdala) showed disproportionate accumulation of amyloid-β_{42} in familial Alzheimer's disease compared to sporadic Alzheimer's disease (Fig. 1B). Although amyloid-β in soluble fractions had more outliers with increased variability, partly because of technical difficulties in quantifying low levels of amyloid-β, these fractions also showed similar cortical and subcortical trends between sporadic and familial Alzheimer's disease (Supplementary Fig. 2 and data not shown). Comparison by regions within sporadic or familial Alzheimer's disease also support region-specific differences in amyloid-β accumulation (Supplementary Fig. 3). Of note, amyloid-β_{42} accumulation

Table 3 Brain regions used for the analysis

Cortical areas		Subcortical areas
Neocortical areas	Limbic areas	
Dorsolateral prefrontal (BA9)	Posterior cingulate (BA31)	Striatum (caudate)
Orbitofrontal (BA12)	Entorhinal (BA28)	Thalamus
Inferior temporal (BA20)	Amygdala*	Hypothalamus
Inferior parietal (BA39/40)		Cerebellum
Primary visual (BA17)		

*Amygdala can also be defined as subcortical areas.
BA = Brodmann area.

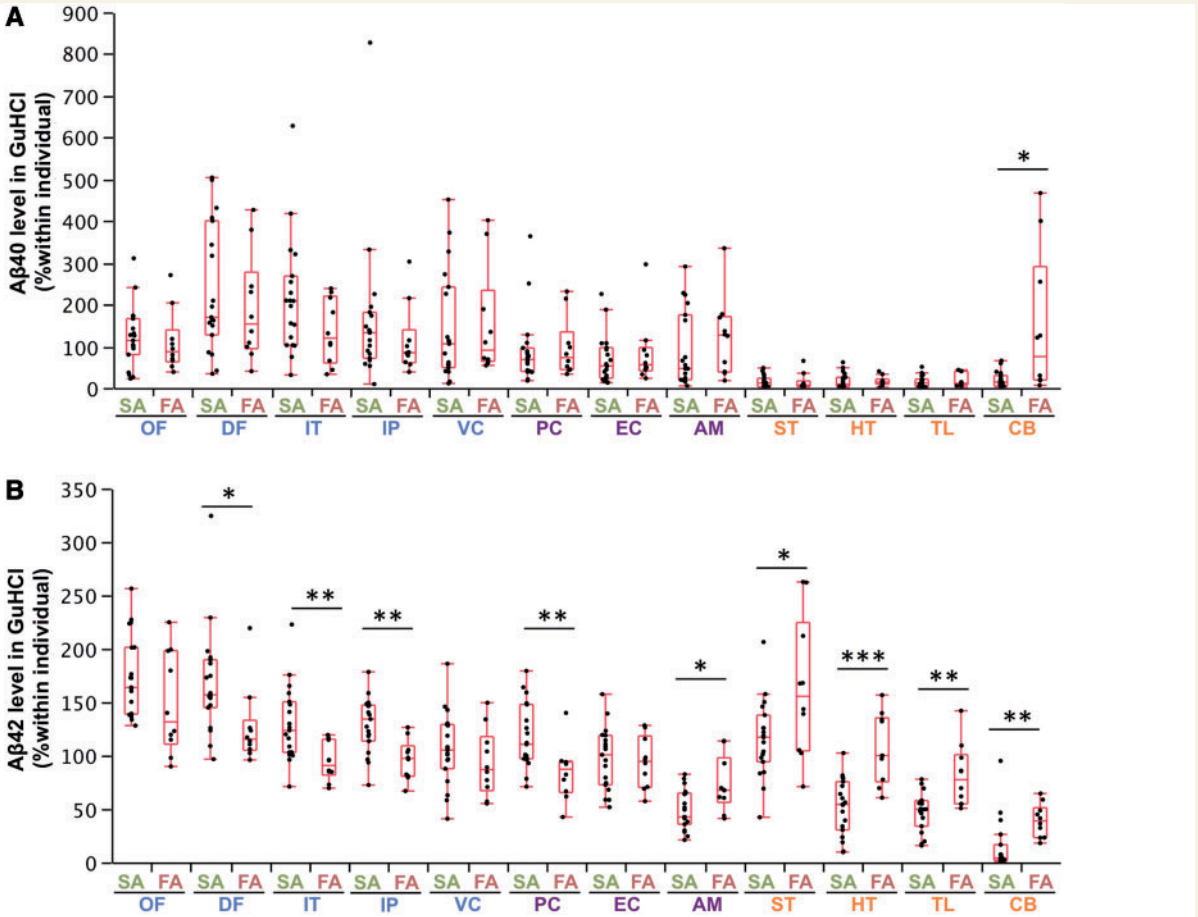

Figure 1 Comparison of accumulated amyloid-β in sporadic and familial Alzheimer's disease in different brain areas. After normalization within each individual, amyloid-β_{40} ($A\beta_{40}$) levels (**A**) and amyloid-β_{42} ($A\beta_{42}$) levels (**B**) in the GuHCl fraction from cases with sporadic or familial Alzheimer's disease are plotted for 12 brain areas with a box-and-whisker diagram. In this and subsequent figures, blue areas = neocortical areas; purple areas = limbic areas; and orange areas = subcortical areas. $^*P < 0.05$, $^{**}P < 0.01$, $^{***}P < 0.001$; Wilcoxon rank-sum test. AM = amygdala; CB = cerebellum; DF = dorsolateral prefrontal cortex; EC = entorhinal cortex; FA = familial Alzheimer's disease; HT = hypothalamus; IP = inferior parietal cortex; IT = inferior temporal cortex; OF = orbitofrontal cortex; PC = posterior cingulate cortex; SA = sporadic Alzheimer's disease; ST = striatum; TL = thalamus; VC = primary visual cortex.

showed a positive regional association with amyloid-β_{40} accumulation in sporadic Alzheimer's disease (Fig. 2A), but not in familial Alzheimer's disease (Fig. 2B).

Regional distribution of molecules related to amyloid-β metabolism in sporadic and familial Alzheimer's disease

We compared the regional distribution of molecules involved in amyloid-β metabolism between sporadic and familial Alzheimer's disease, with the expectation that similar cortical and subcortical changes might be observed. Among these molecules, the regional distribution of apoE in the TX and GuHCl fractions showed cortical to subcortical preference; however, some exceptions were observed for the apoE GuHCl fraction [e.g. temporal cortices (inferior temporal cortex and entorhinal cortex), which exhibited a trend opposite to that of other cortical areas, Fig. 3A and B]. Other molecules did not show a constant cortical to subcortical preference (Supplementary Fig. 4). We also examined regional associations between accumulated amyloid-β and molecules related to amyloid-β metabolism within sporadic and familial Alzheimer's disease (Table 4), as we did previously to assess regional relationships between these molecules in non-demented individuals (Shinohara *et al.*, 2013). PSD95, a post-synaptic marker, showed a strong, positive association with amyloid-β_{42} accumulation in sporadic Alzheimer's disease (also depicted in Fig. 4A), and moderate, positive association with amyloid-β_{42} accumulation in familial Alzheimer's disease (also depicted in Fig. 4B). ApoE in the TX fraction showed a moderate-to-strong inverse association with amyloid-β_{40} and amyloid-β_{42} accumulation in sporadic Alzheimer's disease (also depicted in Fig. 4C) as well as in familial Alzheimer's disease (also depicted in Fig. 4D). On the other hand, apoE in the GuHCl fraction exhibited mild- (though not significant) to-moderate positive association with

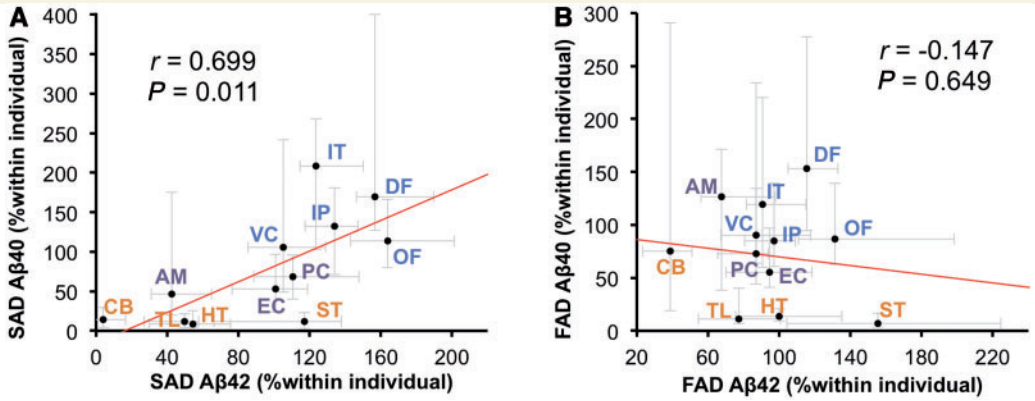

Figure 2 Regional associations between amyloid-β_{40} (Aβ40) and amyloid-β_{42} (Aβ42) in sporadic or familial Alzheimer's disease. (**A**) Amyloid-β_{42} levels in the GuHCl fraction in each brain area of cases with sporadic Alzheimer's disease (SAD) are plotted against amyloid-β_{40} levels in the GuHCl fraction in each brain area of cases with sporadic Alzheimer's disease. (**B**) Amyloid-β_{42} levels in the GuHCl fraction in each brain area of cases with familial Alzheimer's disease (FAD) are plotted against amyloid-β_{40} levels in the GuHCl fraction in each brain area of cases with familial Alzheimer's disease. Values are median with 25 and 75 percentiles. Correlation coefficient (*r*) and *P*-value were acquired by Spearman rank correlation test. AM = amygdala; CB = cerebellum; DF = dorsolateral prefrontal cortex; EC = entorhinal cortex; HT = hypothalamus; IP = inferior parietal cortex; IT = inferior temporal cortex; OF = orbitofrontal cortex; PC = posterior cingulate cortex; ST = striatum; TL = thalamus; VC = primary visual cortex.

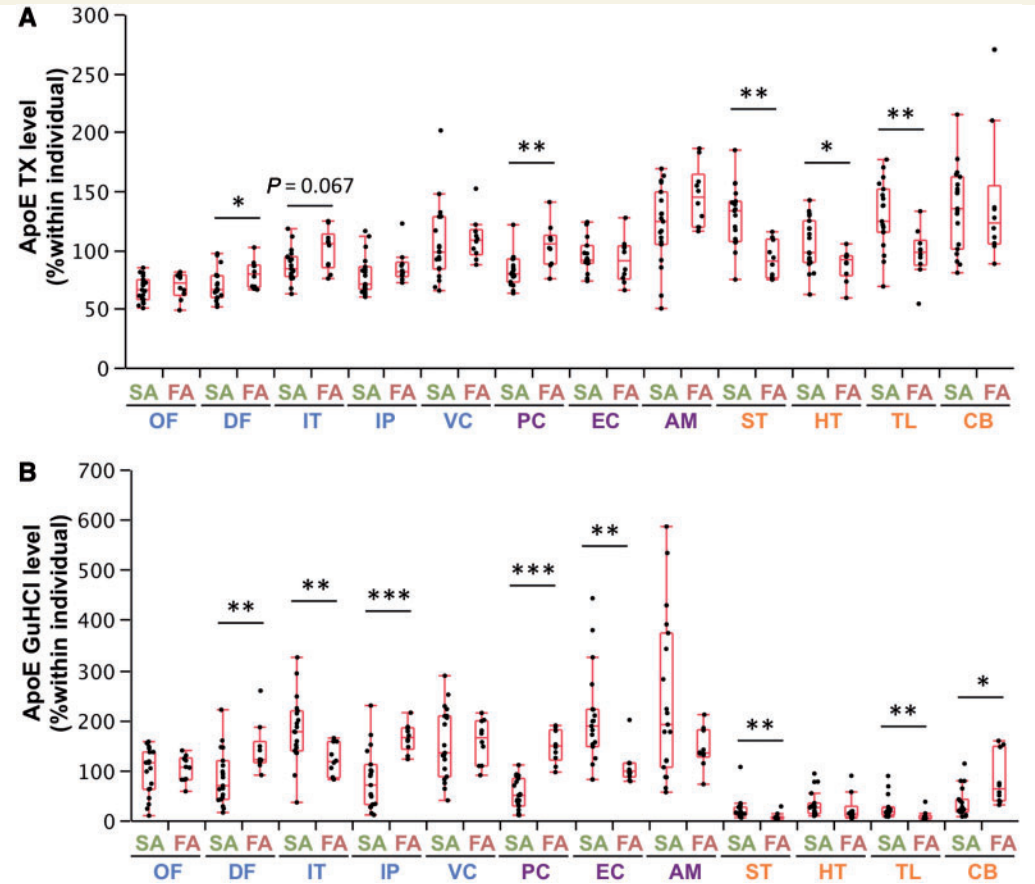

Figure 3 Comparison of molecules related to amyloid-β metabolism between sporadic and familial Alzheimer's disease in different brain areas. After normalization within each individual, levels of apoE in the TX fraction (**A**) and in the GuHCl fraction (**B**) from cases with sporadic or familial Alzheimer's disease are plotted for 12 brain areas with a box-and-whisker diagram. $*P < 0.05$, $**P < 0.01$, $***P < 0.001$; Wilcoxon rank-sum test. AM = amygdala; CB = cerebellum; DF = dorsolateral prefrontal cortex; EC = entorhinal cortex; FA = familial Alzheimer's disease; HT = hypothalamus; IP = inferior parietal cortex; IT = inferior temporal cortex; OF = orbitofrontal cortex; PC = posterior cingulate cortex; SA = sporadic Alzheimer's disease; ST = striatum; TL = thalamus; VC = primary visual cortex.

Table 4 Regional associations between accumulated amyloid-β and molecules related to amyloid-β metabolism within sporadic or familial Alzheimer's disease

	Sporadic Alzheimer's disease				Familial Alzheimer's disease			
	Amyloid-β_{40} GuHCl		Amyloid-β_{42} GuHCl		Amyloid-β_{40} GuHCl		Amyloid-β_{42} GuHCl	
	r	*P*-value	*r*	*P*-value	*r*	*P*-value	*r*	*P*-value
ApoE TBS	**−0.762**	**0.004**	−0.490	0.106	−0.294	0.354	−0.266	0.404
ApoE TX	**−0.741**	**0.006**	**−0.811**	**0.001**	0.140	0.665	**−0.874**	**<0.001**
ApoE GuHCl	0.546	0.067	0.112	0.729	**0.671**	**0.017**	−0.126	0.697
APP	−0.091	0.779	0.546	0.067	−0.084	0.795	0.406	0.191
APP-CTFβ	−0.441	0.152	0.000	1.000	−0.007	0.983	0.371	0.236
BACE1	0.280	0.379	−0.014	0.966	0.566	0.055	−0.203	0.527
PSEN1	−0.021	0.948	0.245	0.443	0.021	0.948	0.042	0.897
NEP	−0.189	0.557	0.000	1.000	−0.357	0.255	0.049	0.880
IDE	0.343	0.276	0.525	0.080	0.182	0.572	0.497	0.101
LRP1	−0.014	0.966	0.301	0.342	0.091	0.779	**0.636**	**0.026**
LDLR	−0.273	0.391	−0.385	0.217	−0.056	0.863	−0.455	0.138
GFAP	**−0.601**	**0.039**	−0.434	0.159	−0.217	0.499	0.098	0.762
SYP	0.497	0.101	0.573	0.051	0.245	0.443	0.259	0.417
PSD95	0.532	0.075	**0.860**	**<0.001**	0.378	0.226	**0.657**	**0.020**

Correlation coefficient (*r*) and *P*-value were acquired by the non-parametric Spearman rank test comparing median value of normalized levels of amyloid-β in the GuHCl fraction with median value of normalized levels of molecules related to amyloid-β metabolism in 19 cases (sporadic Alzheimer's disease) or 10 cases (familial Alzheimer's disease) across 12 brain regions. Significant correlations are shown as bold text.

amyloid-β_{40} accumulation in both sporadic and familial Alzheimer's disease, as shown in Table 4.

We also compared absolute levels of these proteins in cortical areas (average value across cortical areas) among cases with Alzheimer's disease and neurologically normal control subjects, as summarized in Table 5. ApoE in the TX and GuHCl fractions was significantly increased in familial Alzheimer's disease compared to normal ageing and pathological ageing. Specifically, we observed variable levels of apoE in the GuHCl fraction, with familial Alzheimer's disease being the highest, followed by sporadic Alzheimer's disease, pathological ageing and then normal ageing, though there was not a significant difference between sporadic Alzheimer's disease and pathological ageing. Of note, absolute levels of APP, APP-CTFβ, IDE, LRP1, SYP and PSD95 were significantly decreased in both sporadic and familial Alzheimer's disease, compared with normal ageing or pathological ageing. Levels of BACE1, PSEN1 and NEP were also decreased in sporadic Alzheimer's disease, compared with pathological ageing. However, levels of all these proteins, including APP, APP-CTFβ, IDE, LRP1, SYP, PSD95, BACE1, PSEN1 and NEP were not changed in pathological ageing compared to normal ageing. GFAP levels tended to be increased in sporadic and familial Alzheimer's disease, compared with normal or pathological ageing, though these were not significant (Table 5). Significant positive/inverse correlations were also observed among levels of these molecules across all cases (some examples are shown in Supplementary Fig. 5 and summarized in Supplementary Table 2). As some molecules are more abundant in subcortical than cortical areas, we also compared absolute levels of these proteins in subcortical areas among sporadic Alzheimer's disease, familial Alzheimer's disease and neurologically normal controls, and confirmed a similar trend with that of cortical areas (Supplementary Table 3).

Regional associations between accumulated amyloid-β in sporadic or familial Alzheimer's disease and normal distribution of molecules involved in amyloid-β metabolism

The presence of significant neurodegeneration in Alzheimer's disease determines that it is difficult to study a causal relationship between amyloid-β and molecules related to amyloid-β metabolism as the regional pattern of amyloid-β accumulation in Alzheimer's disease is likely formed during the non-demented state (Thal *et al*., 2002; Jack *et al*., 2013). Thus, we next examined the associations between regional distribution of molecules related to amyloid-β metabolism in neurologically normal control subjects without amyloid-β accumulation (i.e. normal ageing) and the pattern of amyloid-β accumulation in sporadic and familial Alzheimer's disease. The regional distribution of molecules related to amyloid-β metabolism in normal controls was similar to that previously reported (Shinohara *et al*., 2013); in brief, although there were a few exceptions, the levels of synapse-related proteins (PSD95, SYP and LRP1 etc.) in neocortical areas were generally higher, followed by limbic areas, and then subcortical areas, whereas the distribution of astrocyte-related proteins (GFAP and apoE) showed opposite trends (Supplementary Fig. 6). The results of the correlation analysis using these molecular distributions are summarized in Table 6. The regional pattern of amyloid-β_{40} accumulation in sporadic Alzheimer's disease showed the strongest (and inverse) association with the normal regional distribution of GFAP (also depicted in Fig. 5A). On the other hand, amyloid-β_{42} accumulation in sporadic Alzheimer's disease showed the strongest (and positive) regional association with normal regional

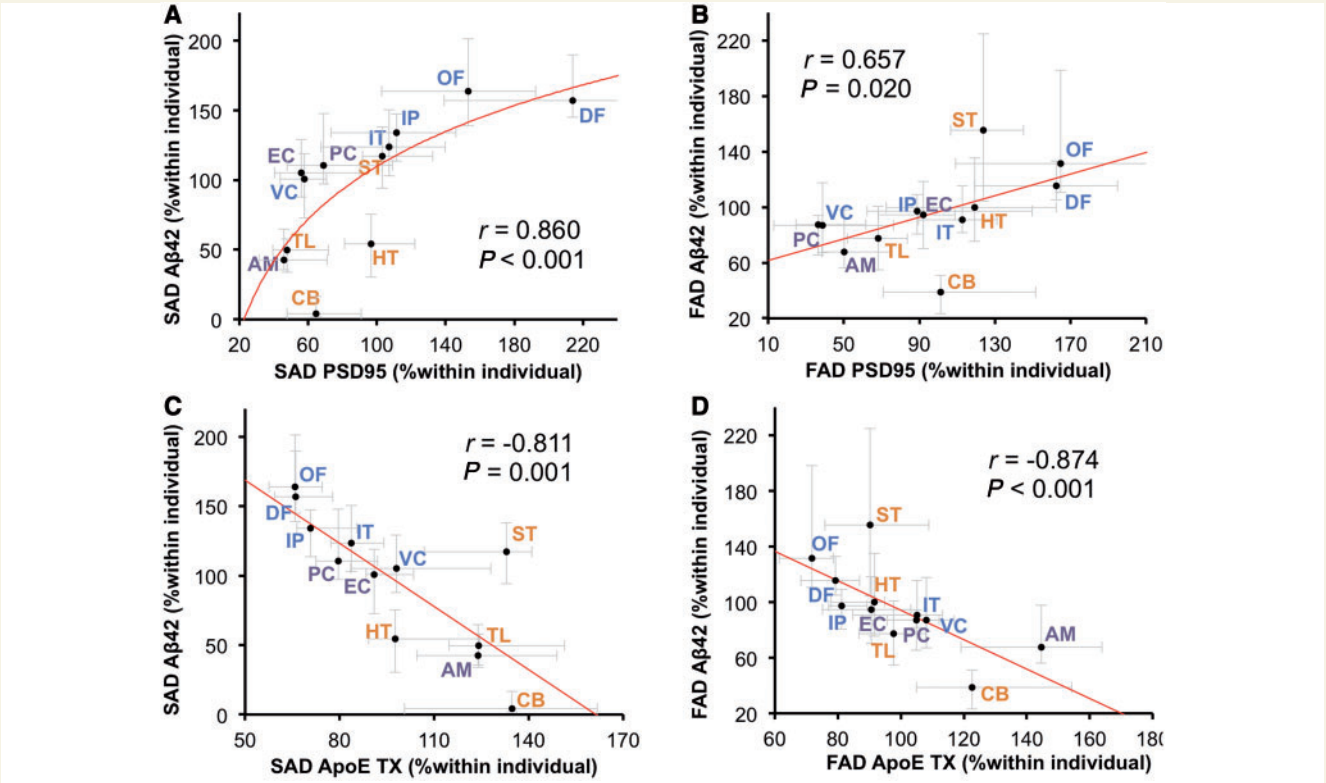

Figure 4 Regional associations between accumulated amyloid-β and PSD95 or apoE in sporadic or familial Alzheimer's disease. (**A**) PSD95 levels in each brain area of cases with sporadic Alzheimer's disease (SAD) are plotted against amyloid-β_{42} (Aβ42) levels in the GuHCl fraction in each brain area of cases with sporadic Alzheimer's disease. (**B**) PSD95 levels in each brain area of cases with familial Alzheimer's disease (FAD) are plotted against amyloid-β_{42} levels in the GuHCl fraction in each brain area of cases with familial Alzheimer's disease. (**C**) ApoE levels in the TX fraction in each brain area of cases with sporadic Alzheimer's disease are plotted against amyloid-β_{42} levels in the GuHCl fraction in each brain area of sporadic Alzheimer's disease cases. (**D**) APOE levels in the TX fraction in each brain area of cases with familial Alzheimer's disease are plotted against amyloid-β_{42} levels in the GuHCl fraction in each brain area of familial Alzheimer's disease cases. Values are median with 25 and 75 percentiles. Correlation coefficient (*r*) and *P*-value were acquired by Spearman rank correlation test. AM = amygdala; CB = cerebellum; DF = dorsolateral prefrontal cortex; EC = entorhinal cortex; HT = hypothalamus; IP = inferior parietal cortex; IT = inferior temporal cortex; OF = orbitofrontal cortex; PC = posterior cingulate cortex; ST = striatum; TL = thalamus VC = primary visual cortex.

Table 5 Comparison of cortical levels of molecules related to amyloid-β metabolism among four studied cohorts

	Normal ageing ($n = 13$)	Pathological ageing ($n = 15$)	Sporadic Alzheimer's disease ($n = 19$)	Familial Alzheimer's disease ($n = 10$)
Cortical apoE TBS (ng/mg)	1157 ± 64	1231 ± 65	1171 ± 53	1225 ± 112
Cortical apoE TX (ng/mg)	1287 ± 104	1291 ± 75	1154 ± 68	2047 ± 170**,#,§§
Cortical apoE GuHCl (ng/mg)	28.6 ± 5.0	148 ± 24*	440 ± 188**	2274 ± 468**,##,§§
Cortical APP (ng/mg)	51.7 ± 5.5	58.4 ± 3.5	32.9 ± 1.9*,##	33.6 ± 1.7*,##
Cortical APP-CTFβ (ng/mg)	0.53 ± 0.03	0.56 ± 0.04	0.34 ± 0.01**,##	0.33 ± 0.02**,##
Cortical BACE1 (ng/mg)	12.9 ± 0.8	14.7 ± 1.0	11.6 ± 0.4#	14.7 ± 0.5§
Cortical PSEN1 (ng/mg)	6.56 ± 0.40	7.80 ± 0.47	5.62 ± 0.33##	6.77 ± 0.43
Cortical NEP (ng/mg)	1.32 ± 0.08	1.36 ± 0.10	1.07 ± 0.06#	1.21 ± 0.07
Cortical IDE (ng/mg)	62.5 ± 7.7	53.1 ± 2.4	30.9 ± 5.1**,#	17.8 ± 4.4**,##
Cortical LRP1 (ng/mg)	45.3 ± 3.3	55.1 ± 4.6	30.2 ± 2.4*,##	29.9 ± 3.1*,##
Cortical LDLR (ng/mg)	0.98 ± 0.06	1.01 ± 0.07	1.02 ± 0.07	1.03 ± 0.12
Cortical GFAP (μg/mg)	822 ± 111	1186 ± 156	1434 ± 168	1546 ± 367
Cortical SYP (ng/mg)	211 ± 10	215 ± 11	167 ± 6*,##	164 ± 7*,##
Cortical PSD95 (ng/mg)	415 ± 40	499 ± 69	194 ± 31*,##	89 ± 18**,##

Values are mean ± SE.
*$P < 0.05$, **$P < 0.01$; compared with normal ageing by *post hoc* Dunn's test.
#$P < 0.05$, ##$P < 0.01$; compared with pathological ageing by *post hoc* Dunn's test.
§$P < 0.05$, §§$P < 0.01$; compared with sporadic Alzheimer's disease by *post hoc* Dunn's test.

Table 6 Regional associations between accumulated amyloid-β in sporadic or familial Alzheimer's disease and molecules related to amyloid-β metabolism in normal ageing

	Sporadic Alzheimer's disease				Familial Alzheimer's disease			
	Amyloid-β_{40} GuHCl		Amyloid-β_{42} GuHCl		Amyloid-β_{40} GuHCl		Amyloid-β_{42} GuHCl	
	r	*P*-value	*r*	*P*-value	*r*	*P*-value	*r*	*P*-value
ApoE TBS	**−0.783**	**0.003**	−0.532	0.075	**−0.580**	**0.048**	−0.007	0.983
ApoE TX	**−0.811**	**0.001**	**−0.720**	**0.008**	**−0.671**	**0.017**	−0.294	0.354
ApoE GuHCl	**−0.713**	**0.009**	**−0.657**	**0.020**	−0.518	0.085	−0.140	0.665
APP	0.217	0.499	**0.664**	**0.019**	−0.014	0.966	**0.832**	**<0.001**
APP-CTFβ	−0.126	0.697	0.406	0.191	−0.322	0.308	**0.783**	**0.003**
BACE1	−0.273	0.391	−0.189	0.557	−0.084	0.795	0.098	0.762
PSEN1	**0.601**	**0.039**	**0.811**	**0.001**	0.112	0.729	**0.580**	**0.048**
NEP	−0.245	0.443	0.028	0.931	−0.469	0.125	0.035	0.914
IDE	**0.888**	**<0.001**	**0.811**	**0.001**	0.511	0.090	0.343	0.276
LRP1	**0.622**	**0.031**	**0.804**	**0.002**	0.315	0.319	**0.692**	**0.013**
LDLR	−0.266	0.404	−0.357	0.255	0.084	0.795	−0.266	0.404
GFAP	**−0.951**	**<0.001**	**−0.615**	**0.033**	**−0.608**	**0.036**	−0.028	0.931
SYP	0.462	0.131	**0.601**	**0.039**	0.021	0.948	0.539	0.071
PSD95	**0.755**	**0.005**	**0.923**	**<0.001**	0.350	0.265	**0.706**	**0.010**

Correlation coefficient (*r*) and *P*-value were acquired by the non-parametric Spearman rank test comparing median value of normalized levels of amyloid-β in the GuHCl fraction in cases with sporadic or familial Alzheimer's disease with median value of normalized levels of molecules related to amyloid-β metabolism in normal ageing cases across 12 brain regions. Significant correlations are shown as bold text.

distribution of PSD95 (also depicted in Fig. 5B). Compared to this association, the regional association between accumulated amyloid-β_{42} in sporadic Alzheimer's disease and the normal distribution of APP was weaker (also depicted in Fig. 5C). Amyloid-β_{40} accumulation in sporadic Alzheimer's disease showed moderate-to-strong negative correlations with normal distribution of apoE in the TBS, TX and GuHCl fractions. The normal regional distributions of GFAP and apoE were inversely associated with amyloid-β_{40} accumulation in familial Alzheimer's disease, as shown in Table 6 and Fig. 5D. These regional associations were also observed within pathological ageing or when comparing amyloid-β accumulation in sporadic Alzheimer's disease with the regional distribution of these molecules in pathological ageing, except for apoE in the GuHCl fraction, which showed a trend of positive (but not significant) regional association with amyloid-β accumulation (Supplementary Table 4). Of note, the regional pattern of amyloid-β_{42} accumulation in familial Alzheimer's disease showed the strongest (and positive) association with the normal regional distribution of APP, whereas the regional association between accumulated amyloid-β_{42} in familial Alzheimer's disease and normal distribution of PSD95 was moderate (also depicted in Fig. 5E and F). Amyloid-β_{42} accumulation in familial Alzheimer's disease also showed similar strong association with normal regional distribution of APP-CTFβ, as shown in Table 6.

Tau accumulation in sporadic and familial Alzheimer's disease

We assessed the regional pattern of tau accumulation. To validate that our tau ELISA was detecting predominantly pathological forms of tau and not normal neuronal tau, we compared the reactivity in the GuHCl fraction between normal controls and sporadic Alzheimer's disease (Supplementary Fig. 7). Tau levels in normal ageing were highest in the entorhinal cortex and amygdala compared to other areas, whereas tau levels in sporadic Alzheimer's disease involved other areas in addition to the entorhinal cortex and amygdala. Indeed, in all brain areas except for the entorhinal cortex and cerebellum, levels of tau in the GuHCl fraction were significantly higher in sporadic Alzheimer's disease than normal ageing. Of note, we observed significant variation in tau levels in the GuHCl fraction in the entorhinal cortex of normal ageing and no significant difference in levels between normal ageing and sporadic Alzheimer's disease, which reflects sensitivity of the ELISA assay to a wide range of tau pathology in the entorhinal cortex of normal ageing as assessed by the Braak neurofibrillary tangles stage (Table 1) (Braak and Braak, 1991). There was a positive correlation between tau levels and Braak stage in the entorhinal and neocortical areas (data not shown). These data demonstrate that tau levels in the GuHCl fraction reflect pathological tau accumulation in the brain.

We then compared tau levels in sporadic and familial Alzheimer's disease. Absolute levels of tau in the GuHCl fraction in familial Alzheimer's disease showed a trend to be higher than sporadic Alzheimer's disease in several areas (Fig. 6A). We also examined whether tau preferentially accumulated in certain regions by comparing individually normalized values, and observed that in familial Alzheimer's disease, tau accumulated more in the orbitofrontal cortex and striatum compared with sporadic Alzheimer's disease, whereas in sporadic Alzheimer's disease, tau accumulated more in the inferior cortex, and with an increased trend in the entorhinal cortex, compared with familial Alzheimer's disease (Fig. 6B). As all familial Alzheimer's disease had Braak stage VI, we compared only sporadic Alzheimer's disease having Braak stage VI with familial Alzheimer's disease (Supplementary Table 5) and found such region-specific tau accumulation persisted (Supplementary Fig. 8).

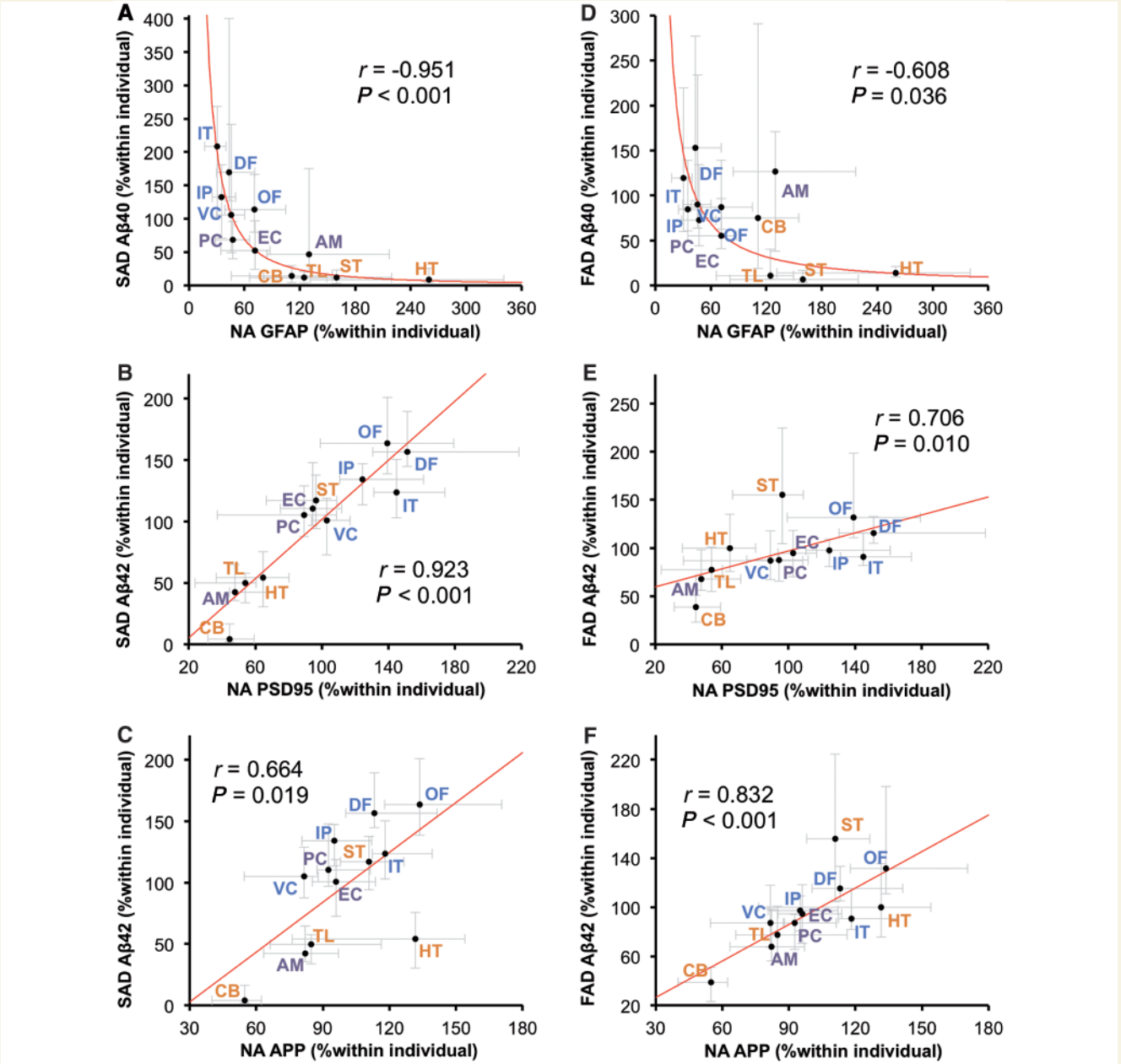

Figure 5 Regional associations between accumulated amyloid-β in sporadic or familial Alzheimer's disease and normal distributions of GFAP, PSD95 or APP. GFAP levels in each brain area of normal ageing (NA) cases are plotted against amyloid-β_{40} (Aβ40) levels in the GuHCl fraction in each brain area of cases with sporadic Alzheimer's disease (SAD; **A**) and cases with familial Alzheimer's disease (FAD; **D**). PSD95 levels in each brain area of normal ageing cases are plotted against amyloid-β_{42} (Aβ42) levels in the GuHCl fraction in each brain area of cases with sporadic Alzheimer's disease (**B**) and cases with familial Alzheimer's disease (**E**). APP levels in each brain area of normal ageing cases are plotted against amyloid-β_{42} levels in the GuHCl fraction in each brain area of cases with sporadic Alzheimer's disease (**C**) and cases with familial Alzheimer's disease (**F**). Values are median with 25 and 75 percentiles. Correlation coefficient (*r*) and *P*-value were acquired by Spearman rank correlation test. AM = amygdala; CB = cerebellum; DF = dorsolateral prefrontal cortex; EC = entorhinal cortex; HT = hypothalamus; IP = inferior parietal cortex; IT = inferior temporal cortex; OF = orbitofrontal cortex; PC = posterior cingulate cortex; ST = striatum; TL = thalamus; VC = primary visual cortex.

We also investigated the relationship of tau in the GuHCl fraction with digital image analysis of tau immunohistochemistry in the striatum with CP13 and PHF1 antibodies, which detect early and late tangle pathology, respectively. Tau levels in the GuHCl fraction of striatum showed a greater correlation with CP13, than PHF1 burden (Fig. 7A and B). When limited to Braak stage VI cases, familial Alzheimer's disease showed higher levels of tau accumulation with CP13 in the striatum, compared with sporadic Alzheimer's disease (Fig. 7C). On the other hand, levels of tau accumulation detected by PHF1 were not statistically

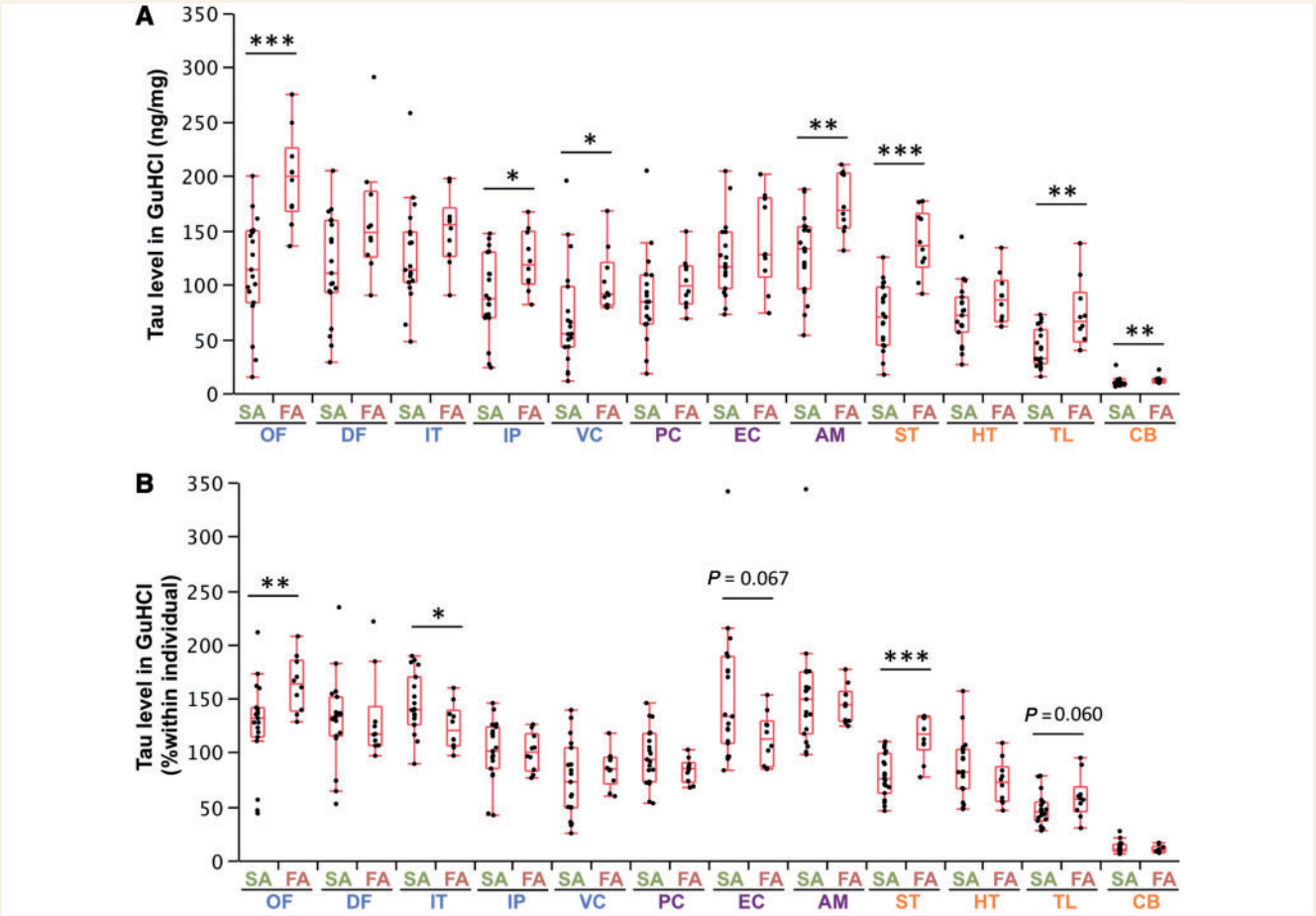

Figure 6 Comparison of accumulated tau in sporadic and familial Alzheimer's disease in different brain areas. (**A**) Tau levels (as absolute value) in the GuHCl fraction from cases with sporadic or familial Alzheimer's disease are plotted for 12 brain areas with a box-and-whisker diagram. (**B**) After normalization within each individual, levels of tau in the GuHCl fraction from cases with sporadic or familial Alzheimer's disease are plotted for 12 brain areas with a box-and-whisker diagram. $*P < 0.05$, $**P < 0.01$, $***P < 0.001$; Wilcoxon rank-sum test. AM = amygdala; CB = cerebellum; DF = dorsolateral prefrontal cortex; EC = entorhinal cortex; FA = familial Alzheimer's disease; HT = hypothalamus; IP = inferior parietal cortex; IT = inferior temporal cortex; OF = orbitofrontal cortex; PC = posterior cingulate cortex; SA = sporadic Alzheimer's disease; ST = striatum; TL = thalamus; VC = primary visual cortex.

different between familial and sporadic Alzheimer's disease (Fig. 7D).

Ante-mortem clinical symptoms

As atypical symptoms, such as pyramidal signs, extrapyramidal signs, dysarthria, myoclonus or seizures, may be more frequent in familial Alzheimer's disease (Rossor *et al*., 1993; Cabrejo *et al*., 2006; Larner and Doran, 2006, 2009), we also retrospectively compared ante-mortem clinical symptoms of familial and sporadic Alzheimer's disease from ante-mortem medical records (Supplementary material). We found that familial Alzheimer's disease showed a significantly increased incidence of pyramidal signs and dysarthria as well as a potentially higher incidence of seizures and myoclonus, but not extrapyramidal signs, compared with sporadic Alzheimer's disease with Braak stage VI (Supplementary Table 6).

Discussion

Mounting evidence indicates that sporadic and familial Alzheimer's disease with autosomal dominant mutations present different clinicopathological features regarding region-specific amyloid-β accumulation, pattern of neurodegeneration, and clinical symptoms. To elucidate the underlying mechanisms that differ between sporadic and familial Alzheimer's disease, we biochemically evaluated amyloid-β accumulation, tau accumulation and molecules related to amyloid-β metabolism across 12 brain regions in post-mortem tissue from sporadic Alzheimer's disease, familial Alzheimer's disease, from neurologically normal control subjects with or without amyloid-β accumulation. We especially focused on the relationship between the normal distribution of key molecules as determined by analyses in normal control subjects and the regional pattern of amyloid-β accumulation in sporadic and familial Alzheimer's disease (Table 6). The rationale for such a comparison is that changes

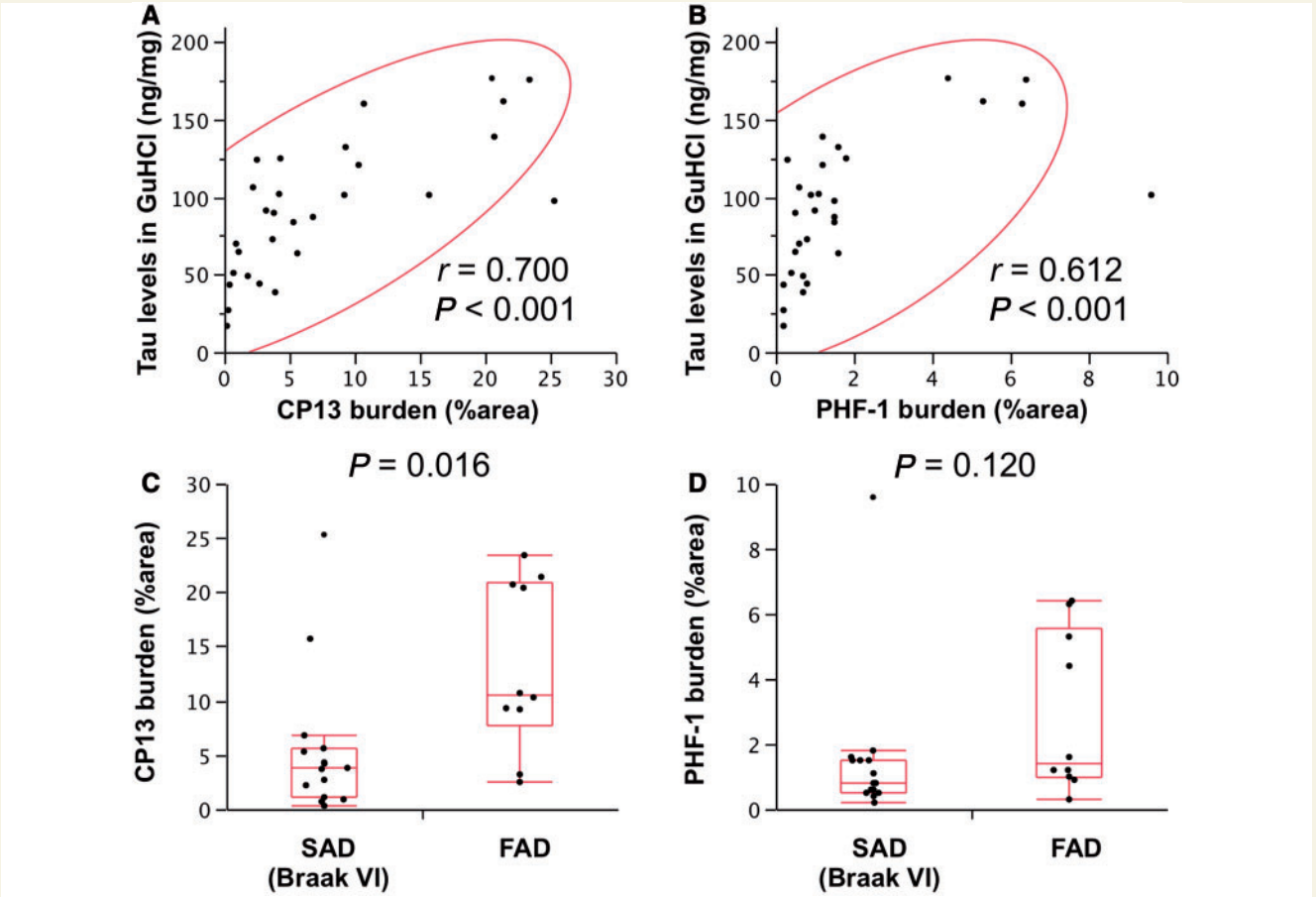

Figure 7 Immunohistochemical analysis of tau in the striatum. Tau levels in the GuHCl fraction in the striatum (caudate) area of cases with total Alzheimer's disease are plotted against CP13 burden (**A**) or PHF1 burden (**B**) in the striatum (putamen) area of cases with total Alzheimer's disease with a 95% probability ellipse (red line). Correlation coefficient (*r*) and *P*-value were acquired by Pearson correlation test. Tau accumulation detected by CP13 (**C**) or PHF1 (**D**) from sporadic Alzheimer's disease (SAD) cases with Braak neurofibrillary tangles VI stage or familial Alzheimer's disease (FAD) cases are plotted with a box-and-whisker diagram. *P*-values were acquired by Wilcoxon rank-sum test.

related to neurodegeneration may mask regional variations when compared to values from cases with only sporadic or familial Alzheimer's disease, as observed in this study. The assumption is that regional differences observed in normal control subjects reflect underlying conditions that contribute to pathology as the disease progresses in the preclinical stages to eventually overtly manifest disease (Thal *et al*., 2002; Buckner *et al*., 2005; Jack *et al*., 2013). In sporadic Alzheimer's disease, amyloid-β_{42} was found to disproportionately accumulate in cortical regions, compared with familial Alzheimer's disease, and to strongly correlate with the normal regional distribution of PSD95. Such a strong regional association between amyloid-β and PSD95 was also observed in our previous study analysing non-demented individuals (Shinohara *et al*., 2013), suggesting that certain forms of synaptic process are strongly involved in the regional specificity of amyloid-β levels (Buckner *et al*., 2005; Vlassenko *et al*., 2010). In contrast, in familial Alzheimer's disease, amyloid-β_{42} was found to disproportionately accumulate in subcortical regions, compared with sporadic Alzheimer's disease, and to correlate strongly with the normal regional distribution of APP and APP-CTFβ. Of note, the regional pattern of amyloid-β_{40} accumulation in cases with both sporadic and familial Alzheimer's disease negatively correlated with the normal regional distribution of apoE (TBS and TX fractions) and GFAP, supporting the protective effects of apoE and astrocytes on amyloid-β accumulation, as previously proposed (Shinohara *et al*., 2013). Interestingly, the striatum showed disproportionate tau accumulation in familial compared to sporadic Alzheimer's disease, which might correlate with striatal dysfunction that underlies some of the atypical neurological features of familial Alzheimer's disease. Taken together with other findings in this study and previous reports, these results suggest that disproportionate cortical amyloid-β_{42} accumulation in sporadic Alzheimer's disease may be related to synapse-mediated effects, while disproportionate subcortical amyloid-β_{42} accumulation in familial Alzheimer's disease may be driven by effects of APP and its processing. We speculate that if tau pathology is downstream of APP/amyloid-β, then the region-specific differences in amyloid-β_{42} accumulation might drive relative differences in tau pathology in

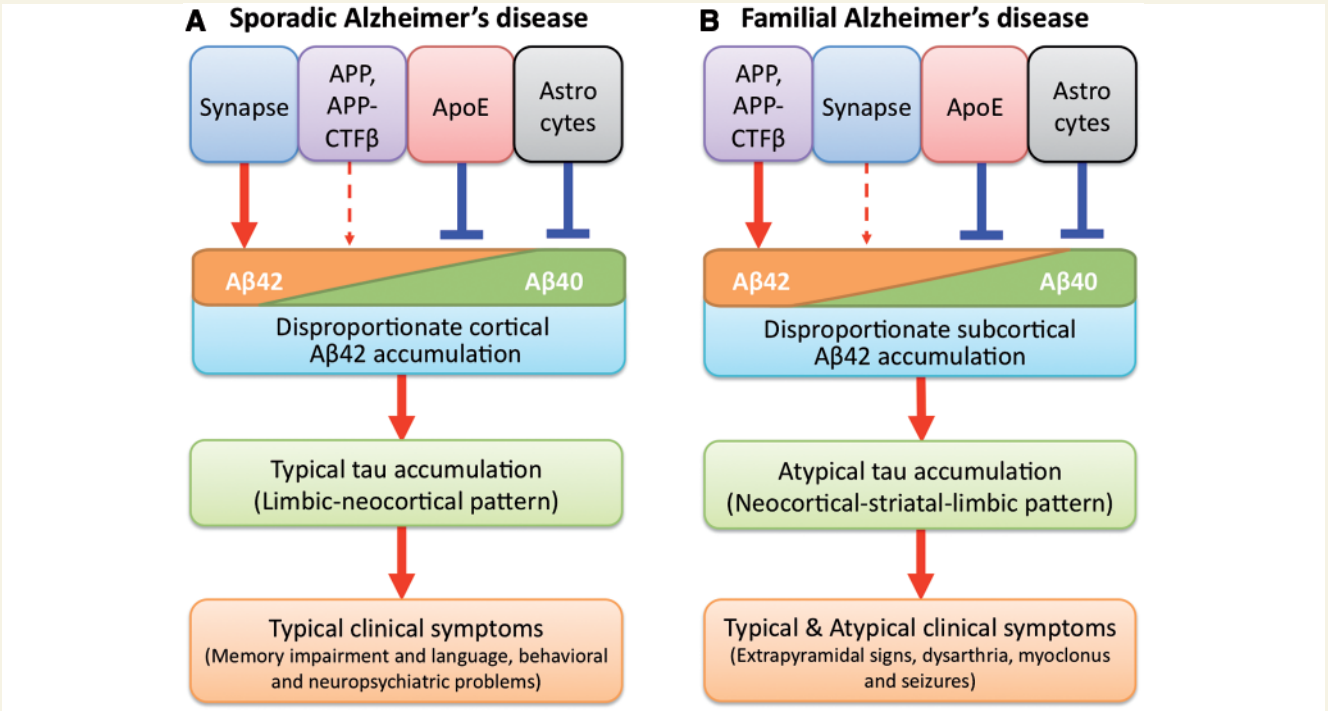

Figure 8 Hypothetical model of pathogenic processes underlying sporadic and familial Alzheimer's disease. In sporadic Alzheimer's disease (**A**), disproportionate amyloid-β_{42} ($A\beta_{42}$) accumulation in cortical areas is driven by synapse-mediated effects, whereas APOE or astrocytes is involved in preventing amyloid-β (especially amyloid-β_{40} ($A\beta_{40}$)) accumulation. In familial Alzheimer's disease (**B**), disproportionate amyloid-β_{42} accumulation in subcortical areas is driven by the effects of APP and its processing, whereas APOE or astrocytes are involved in preventing amyloid-β (especially amyloid-β_{40}) accumulation. The region-specific amyloid-β_{42} accumulation differences drive relative differences in tau pathology in subcortical and cortical areas: typical limbic-neocortical pattern of tau accumulation in sporadic Alzheimer's disease, and atypical neocortical-striatal-limbic pattern of tau accumulation in familial Alzheimer's disease. This difference of tau pathology leads to differences in clinical symptoms, such as extrapyramidal signs, dysarthria, myoclonus or seizures, in familial Alzheimer's disease compared to sporadic Alzheimer's disease.

subcortical and cortical areas, leading to partially distinct clinical symptoms in familial compared to sporadic Alzheimer's disease (Fig. 8).

Despite the widespread knowledge of regional vulnerability to Alzheimer's disease pathology, the underlying mechanism is not fully elucidated, especially in terms of clinicopathological characteristics. Although we previously assessed the regional relationships between amyloid-β and related molecules in non-demented individuals (Shinohara *et al*., 2013), the present study provides the first evidence regarding the strong neuroanatomical associations between amyloid-β and PSD95, APP, apoE and GFAP in Alzheimer's disease brains. Moreover, we observed differences in their neuroanatomical relationships between sporadic and familial Alzheimer's disease. Thus, this study does not only complement our previous study suggesting the pathomechanism of amyloid-β accumulation during the development of sporadic Alzheimer's disease, but provides novel insights into the pathomechanisms underlying distinct clinicopathological features between sporadic and familial Alzheimer's disease.

Recent amyloid imaging studies from several independent groups have demonstrated striatal and thalamic vulnerability to amyloid-β accumulation in familial Alzheimer's disease with various genetic mutations of *APP* or *PSEN1* (Klunk *et al*., 2007; Koivunen *et al*., 2008; Remes *et al*., 2008; Villemagne *et al*., 2009; Knight *et al*., 2011). However, few studies have quantitatively assessed region-specific amyloid-β accumulation in postmortem brains of familial Alzheimer's disease. To our knowledge, this is the first study to biochemically demonstrate striatal and thalamic vulnerability to amyloid-β accumulation in familial, compared to sporadic Alzheimer's disease. In addition, we found disproportionate amyloid-β_{42} accumulation in the amygdala, hypothalamus and cerebellum in familial Alzheimer's disease (Fig. 1). Higher amyloid-β accumulation in the cerebellum of familial Alzheimer's disease was previously observed by an amyloid imaging study (Knight *et al*., 2011). Interestingly, compared to amyloid-β_{42}, amyloid-β_{40} did not show a constant tendency of disproportionate subcortical accumulation in familial Alzheimer's disease, except for the cerebellum (Fig. 1). This result might correspond with a previous study assessing the histopathology of cases with a deletion of exon 9 of *PSEN1* (Koivunen *et al*., 2008). Moreover, regional correlations exist between accumulated amyloid-β_{40} and amyloid-β_{42} in sporadic Alzheimer's disease, but not familial Alzheimer's disease (Fig. 2). These results suggest that different mechanisms exist regarding the accumulation of amyloid-β_{40} and amyloid-β_{42}, at least in familial Alzheimer's disease. Previous studies indicate that amyloid-β_{40} deposition occurs

following the initial deposition of aggregatable amyloid-β_{42}, and thus, amyloid-β_{40} deposition *per se* could be more easily affected by other factors, including APOE and astrocyte-regulated processes (Iwatsubo *et al*., 1994; Gearing *et al*., 1996; Mann *et al*., 1997; Koistinaho *et al*., 2004; Chakrabarty *et al*., 2010). Taken together with other observations in this study, we propose that two opposing effects underlie the respective accumulation of amyloid-β_{42} and amyloid-β_{40} (Fig. 8).

Although an increase in production of amyloid-β_{42} or increased ratio of amyloid-β_{42} to amyloid-β_{40} is clearly implicated in the pathogenesis of familial Alzheimer's disease (Karran *et al*., 2011), it remains unknown how amyloid-β metabolism is disturbed and thus involved in sporadic Alzheimer's disease. Previous clinical imaging studies showed regional overlap between certain forms of neuronal or synaptic activity in neurologically normal subjects and the pattern of amyloid-β accumulation in Alzheimer's disease or cognitively normal elderly subjects with elevated amyloid-β, suggesting synaptic involvement in amyloid-β accumulation (Buckner *et al*., 2005; Vlassenko *et al*., 2010). Our findings would provide additional neuroanatomical evidence of the involvement of such synaptic processes in amyloid-β accumulation in the pathogenesis of sporadic Alzheimer's disease. Moreover, our data suggest that synaptic processes are much more involved in amyloid-β accumulation in sporadic Alzheimer's disease than familial Alzheimer's disease. Previous studies have shown that synapses could regulate amyloid-β production as well as amyloid-β clearance (Shigematsu *et al*., 1992; Takahashi *et al*., 2002; Cirrito *et al*., 2005; Koffie *et al*., 2009; Wu *et al*., 2011). Our data do not exclude either possibility, but suggest that if the same pathway to amyloid-β accumulation is involved as in familial Alzheimer's disease, there should be disproportionate subcortical amyloid-β accumulation. Of note, one sporadic Alzheimer's disease outlier in our study had disproportionate striatal accumulation of amyloid-β_{42} (Fig. 1B). As pathogenic mechanisms could be heterogeneous in sporadic Alzheimer's disease, further characterization of cases with sporadic Alzheimer's disease that have disproportionate subcortical amyloid-β accumulation might provide important insights into heterogeneity of the pathogenic mechanism in sporadic Alzheimer's disease.

Mounting evidence from imaging and CSF biomarker studies suggest that neurodegeneration and neuroinflammation occur after amyloid-β accumulates (Jack *et al*., 2013). We observed a significant change in the absolute levels of several molecules related to amyloid-β metabolism in sporadic and familial Alzheimer's disease compared to normal ageing (Table 5). These changes would be mediated by neurodegeneration or neuroinflammation, as strong correlations were observed among these molecular changes (Supplementary Fig. 5 and Supplementary Table 2) as well as between levels of these molecules and a neuronal marker, neuron-specific enolase (Supplementary Fig. 9). Importantly, these molecular changes would not act as primary mediators of amyloid-β accumulation because pathological ageing did not show such changes, except for APOE (Table 5). Thus, some of the correlations between accumulated amyloid-β and levels of molecules related to amyloid-β metabolism observed in sporadic and familial Alzheimer's disease (Table 4) would include secondary effects due to neurodegeneration or neuroinflammation. In this regard, the results of these correlations should be carefully interpreted considering the degree of neurodegeneration in each cohort. Further analysis comparing cases with Alzheimer's disease at different disease severity might give further clues to understanding the respective mechanisms of neurodegeneration following amyloid-β accumulation. Alternatively, these correlations might also provide insights into the molecular mechanism by which amyloid-β accumulation displays a plateau at the symptomatic phase of Alzheimer's disease (Jack *et al*., 2013). Accordingly, the strong inverse regional correlations between amyloid-β and apoE or GFAP in sporadic/familial Alzheimer's disease cases (Table 4) as well as the opposite cortical and subcortical preference of apoE distribution to that of amyloid-β accumulation (Fig. 3) suggest important roles of apoE or astrocytes in preventing further amyloid-β accumulation at the symptomatic phase of Alzheimer's disease (Akiyama and McGeer, 2004; Shinohara and Bu, 2013).

Of note, apoE in the GuHCl fraction of cases with Alzheimer's disease showed positive regional associations with amyloid-β_{40} accumulation in both sporadic and familial Alzheimer's disease (Table 4). Moreover, the levels of apoE in the TX and GuHCl fractions tended to be higher in sporadic and familial Alzheimer's disease (Table 5). It is well known that apoE co-deposits with various type of amyloid-β plaques, including neuritic plaques, diffuse plaques as well as newly formed plaques (Namba *et al*., 1991; Dickson *et al*., 1997; Nishiyama *et al*., 1997; Thal *et al*., 2002). Such codeposition of apoE with amyloid-β might suggest that apoE promotes amyloid-β accumulation, which is supported by previous *in vitro* and animal experiments (Strittmatter *et al*., 1993; Holtzman *et al*., 2000). However, in addition to amyloid plaques, apoE has been shown to co-deposit with extracellular neurofibrillary tangles, Pick bodies, and prion plaques (Namba *et al*., 1991; Yamaguchi *et al*., 1994; Hayashi *et al*., 1998; Nakamura *et al*., 2000), which suggests that apoE has a strong affinity to amyloid aggregates in general, leading to the accumulation of apoE. Moreover, if the former idea is true, one might expect that sporadic Alzheimer's disease would have more apoE accumulation than familial Alzheimer's disease, as apoE is thought to play an important role in the pathogenesis of sporadic Alzheimer's disease (Bu, 2009). On the other hand, familial Alzheimer's disease often has more prominent co-deposition of apoE with amyloid-β than sporadic Alzheimer's disease (Hesse *et al*., 1999), which is consistent with our finding that patients with familial Alzheimer's disease have higher levels of apoE in the GuHCl fraction than sporadic Alzheimer's disease (Table 5). Taken together, these observations would suggest that apoE prevents amyloid-β accumulation, and during this process, amyloid-β aggregation induces apoE accumulation.

We observed higher levels of tau accumulation in the striatum of familial Alzheimer's disease (Fig. 6A), which is consistent with a previous immunohistochemical study demonstrating higher tau accumulation in the striatum of familial Alzheimer's disease than sporadic Alzheimer's disease (Ringman *et al*., 2011). Disproportionate tau accumulation in the striatum was confirmed after normalization of tau levels within the individual (Fig. 6B) or by comparing familial Alzheimer's disease to sporadic Alzheimer's disease with Braak VI stage (Supplementary Fig. 8). Interestingly, such preferential

accumulation of tau in the striatum reflects CP13 burden more than PHF1 burden (Fig. 7). Tau pathology recognized by CP13 includes early stages of tau accumulation, such as neuritic and pre-tangle pathology, but not extracellular neurofibrillary tangles (Espinoza *et al*., 2008). Recent studies have suggested that early stages of tau accumulation may be more toxic on synaptic function than late stages (Ren and Sahara, 2013; Spillantini and Goedert, 2013). Thus, preferential accumulation of tau in the striatum of familial Alzheimer's disease detected by ELISA in this study may suggest evidence of increased striatal vulnerability to neuronal dysfunction and degeneration in familial Alzheimer's disease, compared to sporadic Alzheimer's disease. Of note, a recent MRI study reported volume loss in the striatum, but not hippocampus, in the presymptomatic stage of familial Alzheimer's disease with various *PSEN1* mutations (Ryan *et al*., 2013). This finding also supports the notion that striatum is a preferential site of neuronal dysfunction and degeneration in familial Alzheimer's disease, accompanied with tau accumulation in the same area.

With regard to the pathophysiological role of tau in Alzheimer's disease, tau accumulation could occur independently of amyloid-β accumulation and dominate neurodegenerative processes in subjects who will develop sporadic Alzheimer's disease (Small and Duff, 2008; Jack *et al*., 2013). Although it is still widely accepted that amyloid-β accumulation would accelerate tau accumulation in Alzheimer's disease, the hypothetical scheme depicted in Fig. 8 thus may be further improved in the future to reflect a potential pathophysiological role of tau accumulation in sporadic Alzheimer's disease. Therefore, further understanding of how tau starts to accumulate in a region-specific manner, as we observed in normal elderly subjects (Supplementary Fig. 7), and then spreads to cortical areas, would be warranted to better understand the pathophysiological processes of Alzheimer's disease.

In addition to typical memory impairment, it is widely known that atypical symptoms such as behaviour disturbance, movement disorders, pyramidal tract signs, myoclonus or seizures frequently occur in familial Alzheimer's disease with *PSEN1* or APP mutations (Rossor *et al*., 1993; Cabrejo *et al*., 2006; Larner and Doran, 2006, 2009). We observed a significantly higher frequency of pyramidal signs and dysarthria as well as potentially increased incidence of seizures and myoclonus, but not extrapyramidal signs, during their disease course, compared to sporadic Alzheimer's disease adjusted by Braak neurofibrillary tangles stage (Supplementary material and Supplementary Table 6). Although it would be difficult to draw a conclusion from this observation because of several limitations, including small number of cases and the retrospective nature of medical record review, it is of note that some atypical symptoms, including extrapyramidal signs, dysarthria, myoclonus and seizure, could be caused by striatal dysfunction (Vercueil and Hirsch, 2002; Chase, 2004; Lalonde and Strazielle, 2012; Pellizzaro Venti *et al*., 2012). Further ante-mortem studies uniformly assessing neurological and psychological features combined with MRI and amyloid and tau PET imaging techniques in a larger cohort of patients with familial Alzheimer's disease is necessary to support the notion that clinical symptoms more frequently observed in familial Alzheimer's disease are a result of disproportionate striatal amyloid and tau accumulation (Fig. 8).

Other potential limitations associated with this study include differences in some demographic characteristics between cases with sporadic and familial Alzheimer's disease, as shown in Table 1. It is well known that such features are very different between sporadic and familial Alzheimer's disease. We also found that it is difficult to choose demographically-matched cases. At least, after matching sporadic and familial Alzheimer's disease cases by disease duration or pathological disease severity (both Braak neurofibrillary tangles stage and synaptic loss), the resulting pattern of amyloid-β accumulation, regional correlations with the normal distribution of other molecules, and the regional pattern of tau accumulation were consistent with our original findings (Supplementary Figs 10 and 11 and Supplementary Tables 7–9). As it is highly possible that heterogenic pathogenic mechanisms in Alzheimer's disease could be confounded by specific genetic mutation, age and *APOE* genotypes, future studies aimed at exploring how these factors affect the observed differences between sporadic and familial Alzheimer's disease would further improve our understanding on the underlying mechanisms.

In summary, the present study provides strong neuropathological evidence for disproportionate cortical amyloid-β_{42} accumulation in sporadic Alzheimer's disease and subcortical amyloid-β_{42} accumulation in familial Alzheimer's disease, which were associated with synaptic markers and APP, respectively. If region-specific amyloid-β_{42} accumulation is mediated by different pathways, it would suggest that underlying aetiologies should be considered in developing more specific therapies to intervene at early stages of the disease processes in Alzheimer's disease.

Acknowledgements

We thank Drs Malcolm Leissring and Samer Abdul-Hay for ELISA reagents detecting IDE, Mr John Gonzalez for assisting with dissection of brain tissues, Ms Caroline Stetler for careful reading of this manuscript, and Drs Steven Younkin, Takahisa Kanekiyo and Henrietta Nielsen and other Bu laboratory members for helpful discussion.

Funding

This research was supported by grants from the National Institutes of Health (NIH) (P01 AG030128-Project 3 and P01 NS074969-Project 3 to G.B.); Alzheimer's Drug Discovery Foundation (ADDF) (to G.B.); American Health Assistance Foundation (AHAF) (to G.B.); Mayo Clinic Alzheimer's Disease Research Centre (ADRC) (P50 AG016574) (to D.W.D and M.S.); Japan Heart Foundation and Naito Foundation (to M.S.). The authors also acknowledge the many individuals who contribute to the Mayo Clinic Alzheimer Disease Research Centre (PI: R.C.P., P50 AG016574) and Mayo Clinic Study on Ageing (PI: R.C.P., U01 AG006786), without whose contributions this study would not have been possible.

Conflict of interest

R.C.P. has been serving as the Chair of a safety monitoring committee for Pfizer (Wyeth) and Janssen Alzheimer Immunotherapy (Elan); and a consultant for Elan Pharmaceuticals and GE Healthcare. All other authors declare that they have no conflicts of interest.

Supplementary material

Supplementary material is available at *Brain* online.

References

Akiyama H, McGeer PL. Specificity of mechanisms for plaque removal after A beta immunotherapy for Alzheimer disease. Nat Med 2004; 10: 117–8.

Bero AW, Yan P, Roh JH, Cirrito JR, Stewart FR, Raichle ME, et al. Neuronal activity regulates the regional vulnerability to amyloid-beta deposition. Nat Neurosci 2011; 14: 750–6.

Braak H, Braak E. Neuropathological stageing of Alzheimer-related changes. Acta Neuropathol 1991; 82: 239–59.

Bu G. Apolipoprotein E and its receptors in Alzheimer's disease: pathways, pathogenesis and therapy. Nat Rev Neurosci 2009; 10: 333–44.

Buckner RL, Snyder AZ, Shannon BJ, LaRossa G, Sachs R, Fotenos AF, et al. Molecular, structural, and functional characterization of Alzheimer's disease: evidence for a relationship between default activity, amyloid, and memory. J Neurosci 2005; 25: 7709–17.

Cabrejo L, Guyant-Marechal L, Laquerriere A, Vercelletto M, De la Fourniere F, Thomas-Anterion C, et al. Phenotype associated with APP duplication in five families. Brain 2006; 129 (Pt 11): 2966–76.

Chakrabarty P, Jansen-West K, Beccard A, Ceballos-Diaz C, Levites Y, Verbeeck C, et al. Massive gliosis induced by interleukin-6 suppresses Aβ deposition *in vivo*: evidence against inflammation as a driving force for amyloid deposition. FASEB J 2010; 24: 548–59.

Chase TN. Striatal plasticity and extrapyramidal motor dysfunction. Parkinsonism Relat Disord 2004; 10: 305–13.

Cirrito JR, Yamada KA, Finn MB, Sloviter RS, Bales KR, May PC, et al. Synaptic activity regulates interstitial fluid amyloid-beta levels *in vivo*. Neuron 2005; 48: 913–22.

Citron M, Oltersdorf T, Haass C, McConlogue L, Hung AY, Seubert P, et al. Mutation of the beta-amyloid precursor protein in familial Alzheimer's disease increases beta-protein production. Nature 1992; 360: 672–4.

Dickson DW, Crystal HA, Mattiace LA, Masur DM, Blau AD, Davies P, et al. Identification of normal and pathological aging in prospectively studied nondemented elderly humans. Neurobiol Aging 1992; 13: 179–89.

Dickson TC, Saunders HL, Vickers JC. Relationship between apolipoprotein E and the amyloid deposits and dystrophic neurites of Alzheimer's disease. Neuropathol Appl Neurobiol 1997; 23: 483–91.

Duering M, Grimm MO, Grimm HS, Schroder J, Hartmann T. Mean age of onset in familial Alzheimer's disease is determined by amyloid beta 42. Neurobiol Aging 2005; 26: 785–8.

Duff K, Eckman C, Zehr C, Yu X, Prada CM, Perez-tur J, et al. Increased amyloid-beta42(43) in brains of mice expressing mutant presenilin 1. Nature 1996; 383: 710–3.

Espinoza M, de Silva R, Dickson DW, Davies P. Differential incorporation of tau isoforms in Alzheimer's disease. J Alzheimers Dis 2008; 14: 1–16.

Gearing M, Mori H, Mirra SS. Abeta-peptide length and apolipoprotein E genotype in Alzheimer's disease. Ann Neurol 1996; 39: 395–9.

Hayashi S, Wakabayashi K, Iwanaga K, Kakita A, Seki K, Tanaka M, et al. Pick's disease: selective occurrence of apolipoprotein E-immunoreactive pick bodies in the limbic system. Acta Neuropathol 1998; 95: 1–4.

Hesse C, Bogdanovic N, Davidsson P, Blennow K. A quantitative and immunohistochemical study on apolipoprotein E in brain tissue in Alzheimer's disease. Dement Geriatr Cogn Disord 1999; 10: 452–9.

Holtzman DM, Fagan AM, Mackey B, Tenkova T, Sartorius L, Paul SM, et al. Apolipoprotein E facilitates neuritic and cerebrovascular plaque formation in an Alzheimer's disease model. Ann Neurol 2000; 47: 739–47.

Iwatsubo T, Odaka A, Suzuki N, Mizusawa H, Nukina N, Ihara Y. Visualization of A beta 42(43) and A beta 40 in senile plaques with end-specific A beta monoclonals: evidence that an initially deposited species is A beta 42(43). Neuron 1994; 13: 45–53.

Jack CR Jr, Knopman DS, Jagust WJ, Petersen RC, Weiner MW, Aisen PS, et al. Tracking pathophysiological processes in Alzheimer's disease: an updated hypothetical model of dynamic biomarkers. Lancet Neurol 2013; 12: 207–16.

Janocko NJ, Brodersen KA, Soto-Ortolaza AI, Ross OA, Liesinger AM, Duara R, et al. Neuropathologically defined subtypes of Alzheimer's disease differ significantly from neurofibrillary tangle-predominant dementia. Acta Neuropathol 2012; 124: 681–92.

Karran E, Mercken M, Strooper BD. The amyloid cascade hypothesis for Alzheimer's disease: an appraisal for the development of therapeutics. Nat Rev Drug Discov 2011; 10: 698–712.

Klunk WE, Price JC, Mathis CA, Tsopelas ND, Lopresti BJ, Ziolko SK, et al. Amyloid deposition begins in the striatum of presenilin-1 mutation carriers from two unrelated pedigrees. J Neurosci 2007; 27: 6174–84.

Knight WD, Okello AA, Ryan NS, Turkheimer FE, Rodriguez Martinez de Llano S, Edison P, et al. Carbon-11-Pittsburgh compound B positron emission tomography imaging of amyloid deposition in presenilin 1 mutation carriers. Brain 2011; 134 (Pt 1): 293–300.

Koffie RM, Meyer-Luehmann M, Hashimoto T, Adams KW, Mielke ML, Garcia-Alloza M, et al. Oligomeric amyloid beta associates with postsynaptic densities and correlates with excitatory synapse loss near senile plaques. Proc Natl Acad Sci USA 2009; 106: 4012–7.

Koistinaho M, Lin S, Wu X, Esterman M, Koger D, Hanson J, et al. Apolipoprotein E promotes astrocyte colocalization and degradation of deposited amyloid-beta peptides. Nat Med 2004; 10: 719–26.

Koivunen J, Verkkoniemi A, Aalto S, Paetau A, Ahonen J-P, Viitanen M, et al. PET amyloid ligand [11C]PIB uptake shows predominantly striatal increase in variant Alzheimer's disease. Brain 2008; 131: 1845–53.

Kumar-Singh S, Theuns J, Van Broeck B, Pirici D, Vennekens K, Corsmit E, et al. Mean age-of-onset of familial alzheimer disease caused by presenilin mutations correlates with both increased Abeta42 and decreased Abeta40. Hum Mutat 2006; 27: 686–95.

Lalonde R, Strazielle C. Brain regions and genes affecting myoclonus in animals. Neurosci Res 2012; 74: 69–79.

Larner AJ, Doran M. Clinical phenotypic heterogeneity of Alzheimer's disease associated with mutations of the presenilin-1 gene. J Neurol 2006; 253: 139–58.

Larner AJ, Doran M. Genotype-phenotype relationships of presenilin-1 mutations in Alzheimer's disease: an update. J Alzheimers Dis 2009; 17: 259–65.

Lee GJ, Lu PH, Medina LD, Rodriguez-Agudelo Y, Melchor S, Coppola G, et al. Regional brain volume differences in symptomatic and presymptomatic carriers of familial Alzheimer's disease mutations. J Neurol Neurosurg Psychiatry 2013; 84: 154–62.

Mann DM, Iwatsubo T, Pickering-Brown SM, Owen F, Saido TC, Perry RH. Preferential deposition of amyloid beta protein (Abeta) in the form Abeta40 in Alzheimer's disease is associated with a gene dosage effect of the apolipoprotein E E4 allele. Neurosci Lett 1997; 221: 81–4.

Nakamura S, Ono F, Hamano M, Odagiri K, Kubo M, Komatsuzaki K, et al. Immunohistochemical detection of apolipoprotein E within

prion-associated lesions in squirrel monkey brains. Acta Neuropathol 2000; 100: 365–70.
Namba Y, Tomonaga M, Kawasaki H, Otomo E, Ikeda K. Apolipoprotein E immunoreactivity in cerebral amyloid deposits and neurofibrillary tangles in Alzheimer's disease and kuru plaque amyloid in Creutzfeldt-Jakob disease. Brain Res 1991; 541: 163–6.
Nishiyama E, Iwamoto N, Ohwada J, Arai H. Distribution of apolipoprotein E in senile plaques in brains with Alzheimer's disease: investigation with the confocal laser scan microscope. Brain Res 1997; 750: 20–4.
Pellizzaro Venti M, Paciaroni M, Caso V. Caudate infarcts and hemorrhages. Front Neurol Neurosci 2012; 30: 137–40.
Remes AM, Laru L, Tuominen H, Aalto S, Kemppainen N, Mononen H, et al. Carbon 11-labeled pittsburgh compound B positron emission tomographic amyloid imaging in patients with APP locus duplication. Arch Neurol 2008; 65: 540–4.
Ren Y, Sahara N. Characteristics of tau oligomers. Front Neurol 2013; 4: 102.
Ringman JM, Gylys KH, Medina LD, Fox M, Kepe V, Flores DL, et al. Biochemical, neuropathological, and neuroimaging characteristics of early-onset Alzheimer's disease due to a novel PSEN1 mutation. Neurosci Lett 2011; 487: 287–92.
Rossor MN, Newman S, Frackowiak RS, Lantos P, Kennedy AM. Alzheimer's disease families with amyloid precursor protein mutations. Ann N Y Acad Sci 1993; 695: 198–202.
Rovelet-Lecrux A, Hannequin D, Raux G, Le Meur N, Laquerriere A, Vital A, et al. APP locus duplication causes autosomal dominant early-onset Alzheimer disease with cerebral amyloid angiopathy. Nat Genet 2006; 38: 24–6.
Rowe CC, Ng S, Ackermann U, Gong SJ, Pike K, Savage G, et al. Imaging beta-amyloid burden in aging and dementia. Neurology 2007; 68: 1718–25.
Ryan NS, Keihaninejad S, Shakespeare TJ, Lehmann M, Crutch SJ, Malone IB, et al. Magnetic resonance imaging evidence for presymptomatic change in thalamus and caudate in familial Alzheimer's disease. Brain 2013; 136 (Pt 5): 1399–414.
Scheuner D, Eckman C, Jensen M, Song X, Citron M, Suzuki N, et al. Secreted amyloid beta-protein similar to that in the senile plaques of Alzheimer's disease is increased *in vivo* by the presenilin 1 and 2 and APP mutations linked to familial Alzheimer's disease. Nat Med 1996; 2: 864–70.
Shigematsu K, McGeer PL, McGeer EG. Localization of amyloid precursor protein in selective postsynaptic densities of rat cortical neurons. Brain Res 1992; 592: 353–7.
Shinohara M, Bu G. What can we learn from regional vulnerability to amyloid-β accumulation in nondemented individuals? Neurodegener Dis Manag 2013; 3: 187–9.
Shinohara M, Petersen RC, Dickson DW, Bu G. Brain regional correlation of amyloid-beta with synapses and apolipoprotein E in non-demented individuals: potential mechanisms underlying regional vulnerability to amyloid-beta accumulation. Acta Neuropathol 2013; 125: 535–47.
Small SA, Duff K. Linking Abeta and tau in late-onset Alzheimer's disease: a dual pathway hypothesis. Neuron 2008; 60: 534–42.
Spillantini MG, Goedert M. Tau pathology and neurodegeneration. Lancet Neurol 2013; 12: 609–22.
Strittmatter WJ, Weisgraber KH, Huang DY, Dong LM, Salvesen GS, Pericak-Vance M, et al. Binding of human apolipoprotein E to synthetic amyloid beta peptide: isoform-specific effects and implications for late-onset Alzheimer disease. Proc Natl Acad Sci USA 1993; 90: 8098–102.
Takahashi RH, Milner TA, Li F, Nam EE, Edgar MA, Yamaguchi H, et al. Intraneuronal Alzheimer abeta42 accumulates in multivesicular bodies and is associated with synaptic pathology. Am J Pathol 2002; 161: 1869–79.
Thal DR, Rub U, Orantes M, Braak H. Phases of A beta-deposition in the human brain and its relevance for the development of AD. Neurology 2002; 58: 1791–800.
Thies W, Bleiler L. Alzheimer's disease facts and figures. Alzheimers Dement 2013; 9: 208–45.
Thinakaran G, Koo EH. Amyloid precursor protein trafficking, processing, and function. J Biol Chem 2008; 283: 29615–9.
Vercueil L, Hirsch E. Seizures and the basal ganglia: a review of the clinical data. Epileptic Disord 2002; 4: S47–54.
Villemagne VL, Ataka S, Mizuno T, Brooks WS, Wada Y, Kondo M, et al. High striatal amyloid beta-peptide deposition across different autosomal Alzheimer disease mutation types. Arch Neurol 2009; 66: 1537–44.
Vlassenko AG, Vaishnavi SN, Couture L, Sacco D, Shannon BJ, Mach RH, et al. Spatial correlation between brain aerobic glycolysis and amyloid-beta (Abeta) deposition. Proc Natl Acad Sci USA 2010; 107: 17763–7.
Wojtas A, Heggeli KA, Finch N, Baker M, DeJesus-Hernandez M, Younkin SG, et al. C9ORF72 repeat expansions and other FTD gene mutations in a clinical AD patient series from Mayo Clinic. Am J Neurodegener Dis 2012; 1: 107–18.
Wu J, Petralia RS, Kurushima H, Patel H, Jung MY, Volk L, et al. Arc/Arg3.1 regulates an endosomal pathway essential for activity-dependent beta-amyloid generation. Cell 2011; 147: 615–28.
Yamaguchi H, Ishiguro K, Sugihara S, Nakazato Y, Kawarabayashi T, Sun X, et al. Presence of apolipoprotein E on extracellular neurofibrillary tangles and on meningeal blood vessels precedes the Alzheimer beta-amyloid deposition. Acta Neuropathol 1994; 88: 413–9.